Supplementary Fig. 1

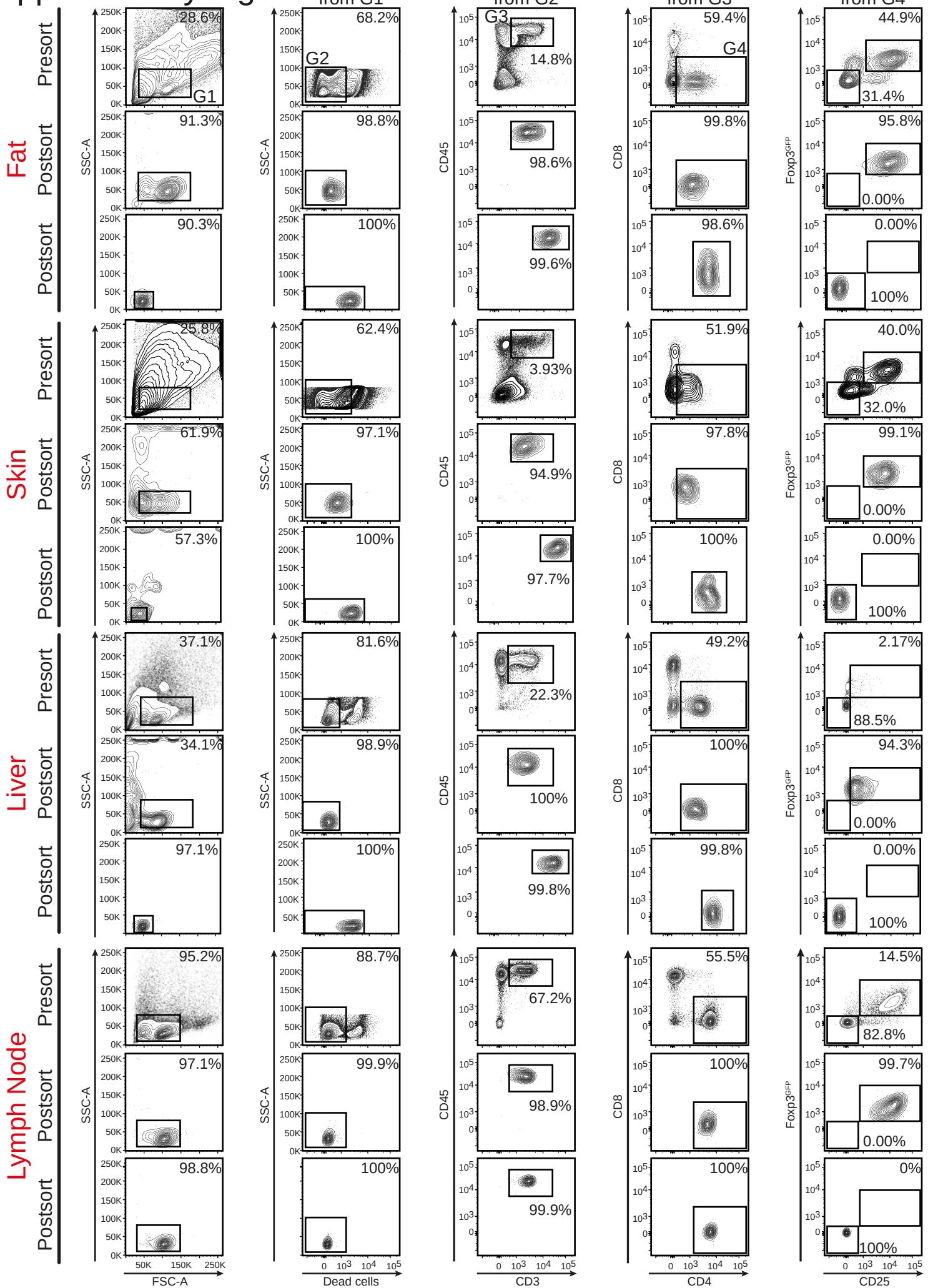

Supplementary Figure 1. Sorting scheme and post-sort quality control of tissue T cells. This supplementary figure is an extension of **Figure 1.** Presort gating scheme for T_{reg} cells and T_{conv} cells from fat, skin, liver, and inguinal LN, including a post-sort re-acquisition of samples as quality control measure. Cells were gated as indicated. Numbers indicate percent of cells per gate.

Supplementary Fig. 2

a

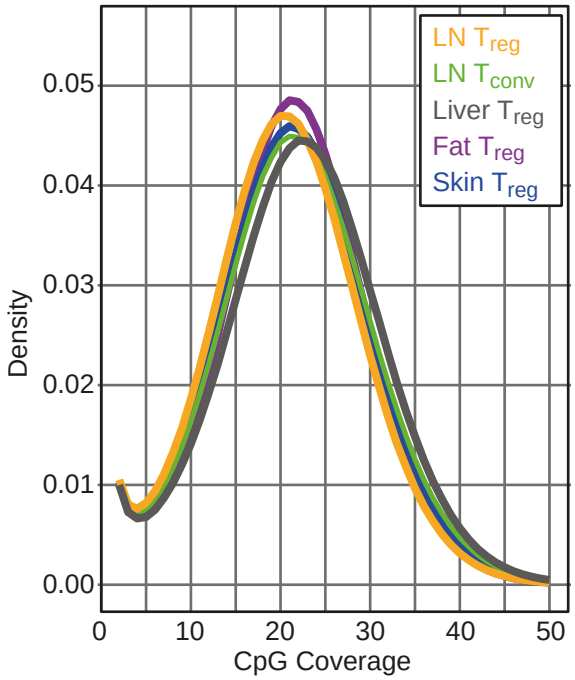

b

20% cutoff

	Liver T_{reg}	LN T_{conv}	LN T_{reg}	Skin T_{reg}	
Liver T_{reg}	2273	9231	4540	656	Fat T_{reg}
LN T_{conv}	4072	343	1696		Liver T_{reg}
LN T_{reg}		1439	9081		LN T_{conv}
Skin T_{reg}			3883		LN T_{reg}

30% cutoff

	Liver T_{reg}	LN T_{conv}	LN T_{reg}	Skin T_{reg}	
Liver T_{reg}	581	4404	1593	127	Fat T_{reg}
LN T_{conv}	1194	31	482		Liver T_{reg}
LN T_{reg}		339	4615		LN T_{conv}
Skin T_{reg}			1645		LN T_{reg}

40% cutoff

	Liver T_{reg}	LN T_{conv}	LN T_{reg}	Skin T_{reg}	
Liver T_{reg}	98	1465	394	18	Fat T_{reg}
LN T_{conv}	261	9	93		Liver T_{reg}
LN T_{reg}		91	1647		LN T_{conv}
Skin T_{reg}			418		LN T_{reg}

c

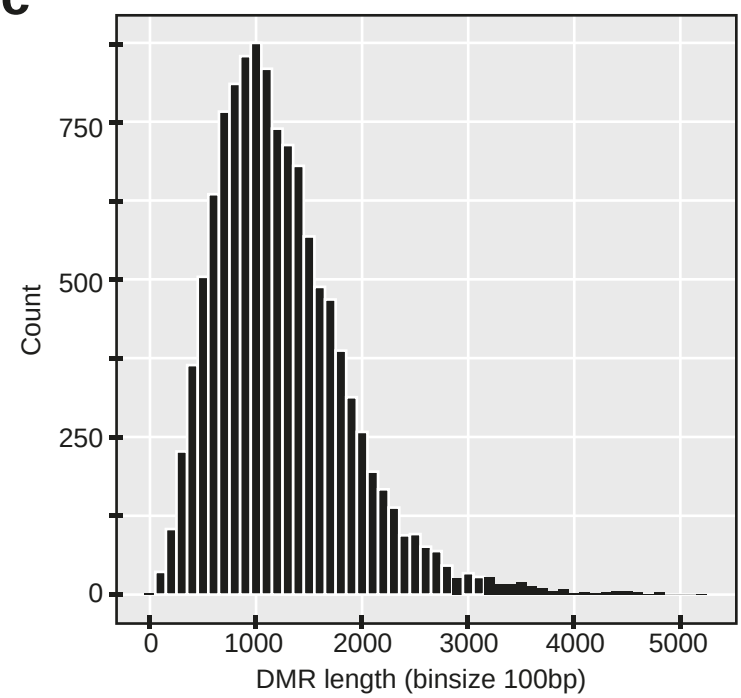

d

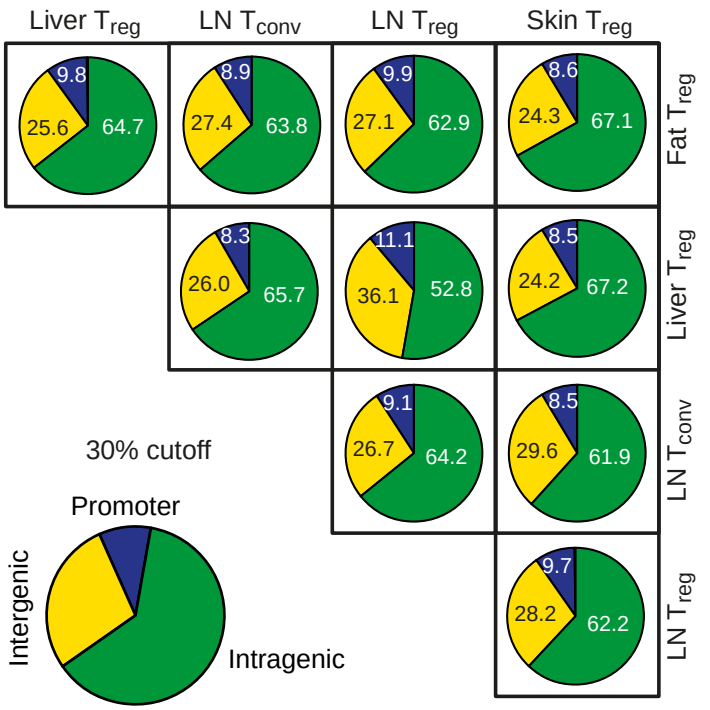

Supplementary Figure 2. Coverage, frequency, length distribution, and functional classification of DMRs. (**a**) CpG coverage of whole-genome methylation data from three replicates of LN T_{reg} (yellow), LN T_{conv} (green), liver T_{reg} (grey), fat T_{reg} (purple), and skin T_{reg} (blue) cells. (**b**) Number of DMRs for 20%, 30%, and 40% cutoff in methylation change. Numbers are derived from pairwise comparisons of indicated groups. At least 30% difference in DNA methylation was chosen for further analysis (30% cutoff). (**c**) DMR length distribution for all DMRs with at least 30% change in methylation is displayed, with a binsize of 100 base pairs. (**d**) The DMR localization (promoter, intragenic, intragenic) for all pairwise comparisons was identified (30% cutoff).

Supplementary Fig. 3

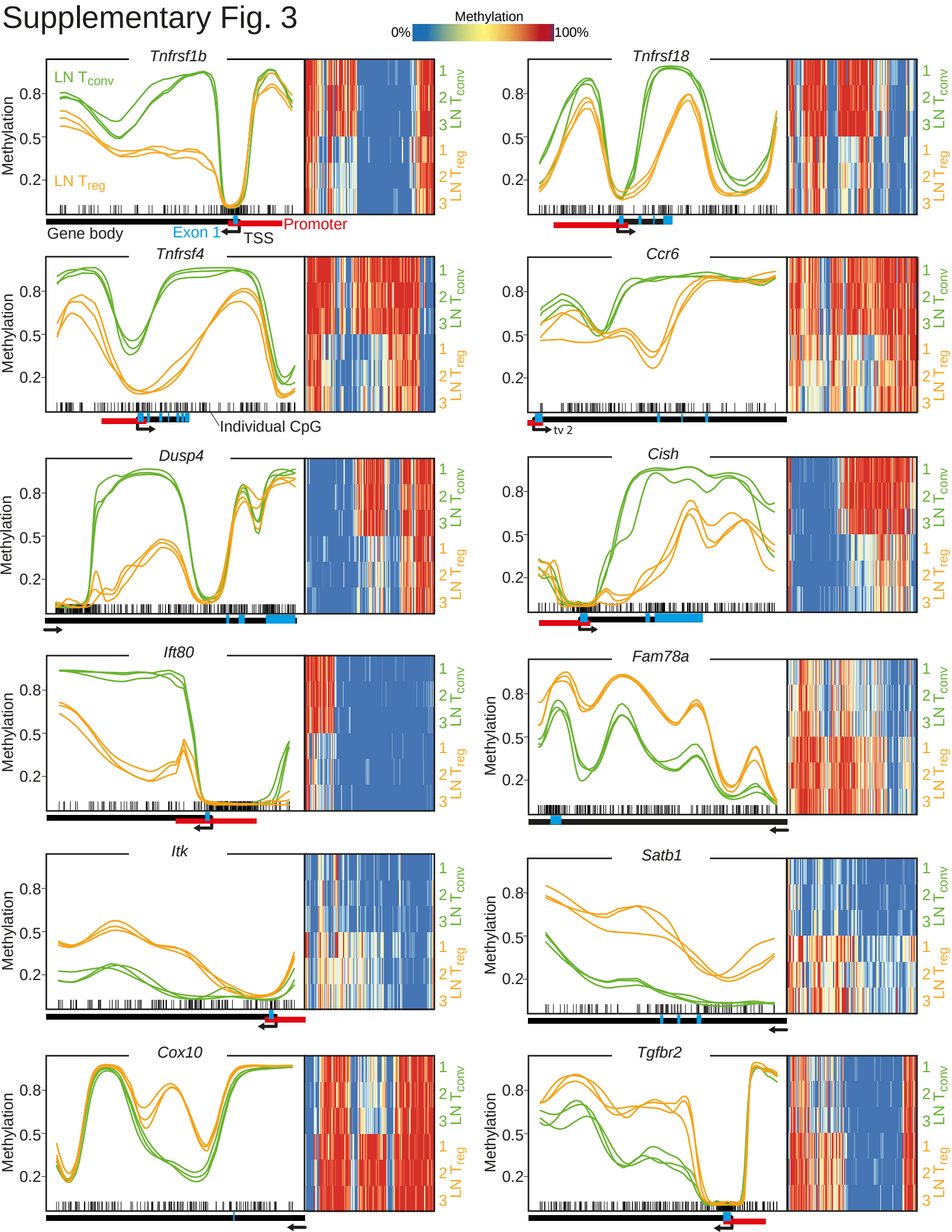

Supplementary Figure 3. Detailed overview of common T_{reg}-specific demethylated or methylated regions. This supplementary figure is an extension of **Figure 3.** Selected genes identified as hypomethylated or hypermethylated in T_{reg} cells are plotted, for both LN T_{reg} (yellow lines) and LN T_{conv} (green lines). Each line represents one replicate (n=3). The precise genomic localization of the DMRs can be found in **supplementary Table 1**. The left-hand part of each plot is a smoothed graphical representation of CpG methylation. Methylation levels are beta values ranging from 0 (unmethylated) to 1 (methylated). The attached right panel represents the methylation heat map of all individual CpGs, indicated as little ticks at the bottom of each plot. The methylation status of CpGs is indicated by color-code (blue = unmethylated to red = methylated). Gene body, promoter, TSS and exon structures are annotated below the graph. Arrows indicate gene direction, black bars gene body regions, red bars annotate promoter regions, blue bars exons. We plot *Tnfrsf1b* (Tumor necrosis factor receptor superfamily member 1B; TNFR2; CD120b), *Tnfrsf18* (Tumor necrosis factor receptor superfamily member 18; AITR; GITR; CD357), *Tnfrsf4* (Tumor necrosis factor receptor superfamily member 4; CD134; OX-40), *Ccr6* (Chemokine receptor 6; CD196; tv2 = transcript variant 2), *Dusp4* (Dual specificity protein phosphatase 4), *Cish* (Cytokine-inducible SH2-containing protein), *Ift80* (Intraflagellar transport protein 80 homolog), *Fam78a* (Family with Sequence Similarity 78-Member A), *Itk* (Tyrosine-protein kinase ITK/TSK; Interleukin-2-inducible T-cell kinase), *Satb1* (Special AT-rich sequence-binding protein-1), *Cox10* (Protoheme IX farnesyltransferase, mitochondrial; Cytochrome c oxidase 10), *Tgfbr2* (Transforming growth factor, beta receptor II).

Supplementary Fig. 4

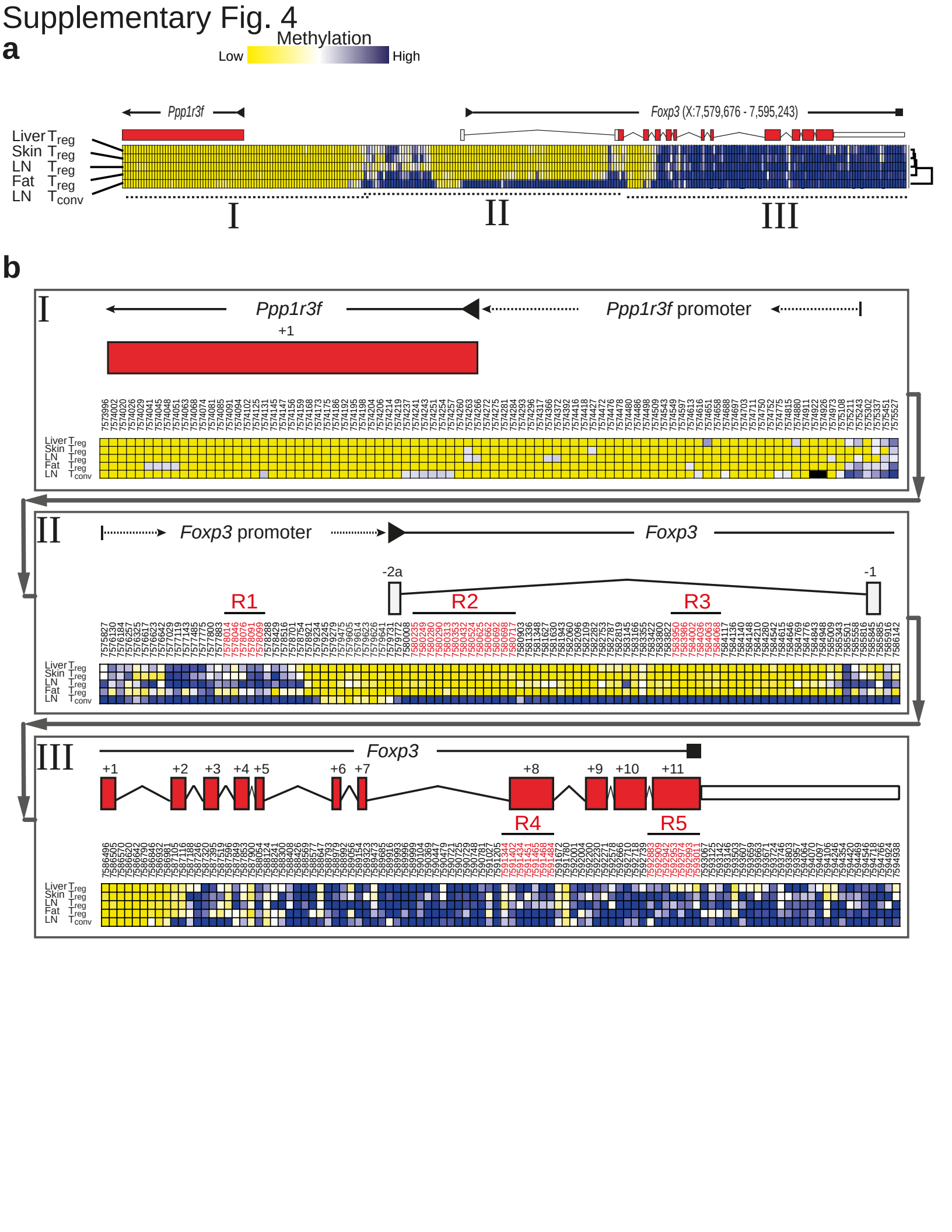

Supplementary Figure 4. Detailed overview of CpG methylation at the *Foxp3* gene. This supplementary figure is an extension of **Figure 3.** (**a**) Heatmap depicting CpG methylation from ChrX:7,579,676-7,595,243 (Mm10) for liver T_{reg}, skin T_{reg}, LN T_{reg}, Fat T_{reg} and LN T_{conv}. Intron and exon structures for the *Ppp1r3f* and *Foxp3* gene are superimposed. Blue color indicates high methylation, yellow low methylation. (**b**) Same heat map as in (**a**), but enlarged and with annotated genomic locations of CG dinucleotides as numbers above. Indicated in red are regions (R1-R5) used for amplicon-based sequencing of bisulfite-converted DNA.

Supplementary Fig. 5

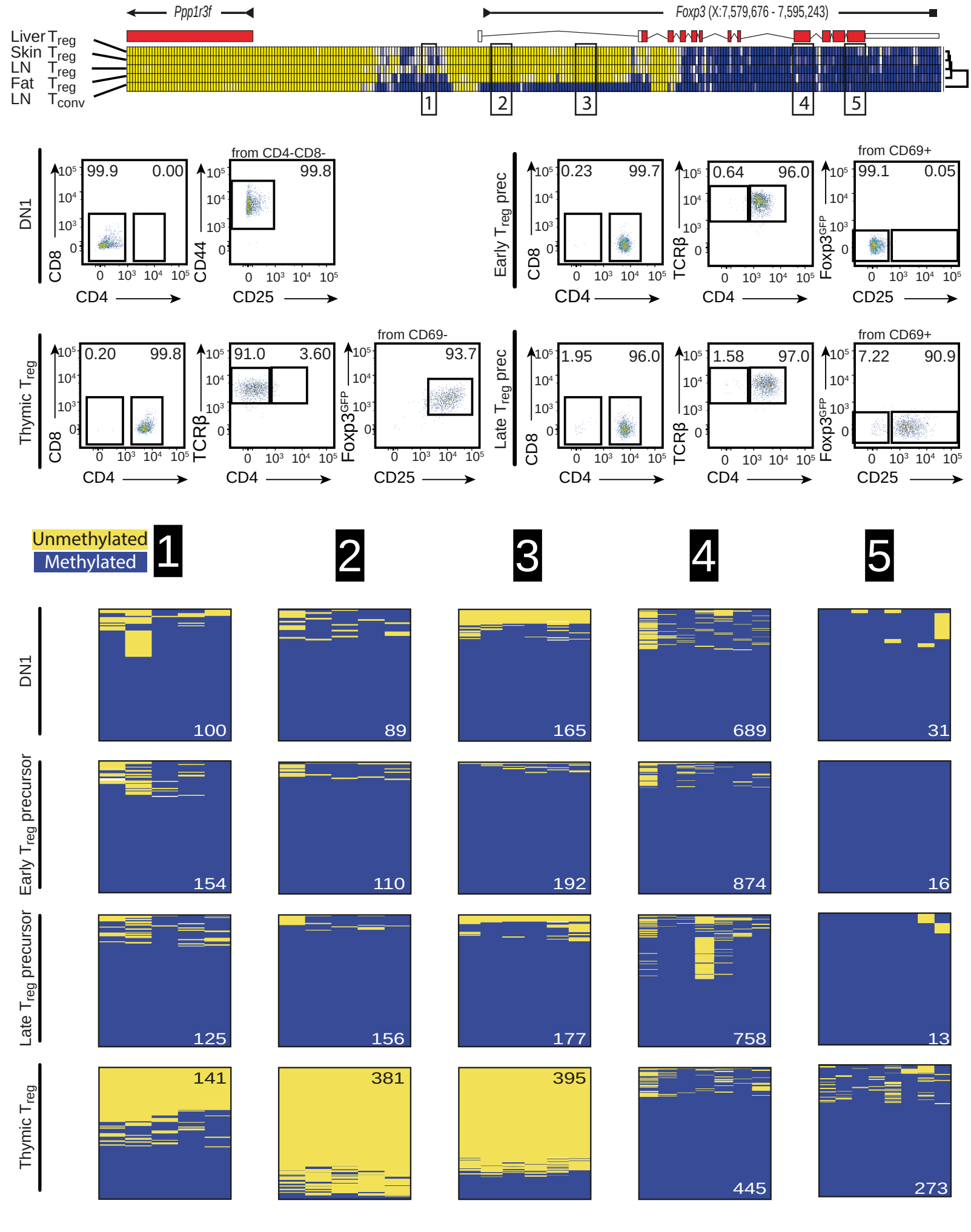

Supplementary Figure 5. Analysis of *Foxp3* CpG methylation during T_{reg} development. This supplementary figure is an extension of **Figure 3.** On top, overview of *Foxp3* gene methylation status based on TWGBS data. Below, post-sort quality control of target cell populations. We isolated double negative 1 (DN1) thymocytes ($CD4^-CD8^-CD25^-CD44^+$), early thymic T_{reg} precursors ($CD4^+CD8^-TCRb^+CD69^+CD25^-Foxp3(GFP)^-$), late thymic T_{reg} precursors ($CD4^+CD8^-TCRb^+ CD69^+CD25^+Foxp3(GFP)^-$), and mature thymus T_{reg} cells ($CD4^+CD8^-TCRb^+CD69^-CD25^+Foxp3(GFP)^+$). Results of 454 pyrosequencing for all T cell populations and regions are shown below, where colors indicate methylation status of the individual CpG sites. Yellow represents unmethylated and blue methylated CpG, while numbers depict quantity of analyzed reads.

Supplementary Fig. 6

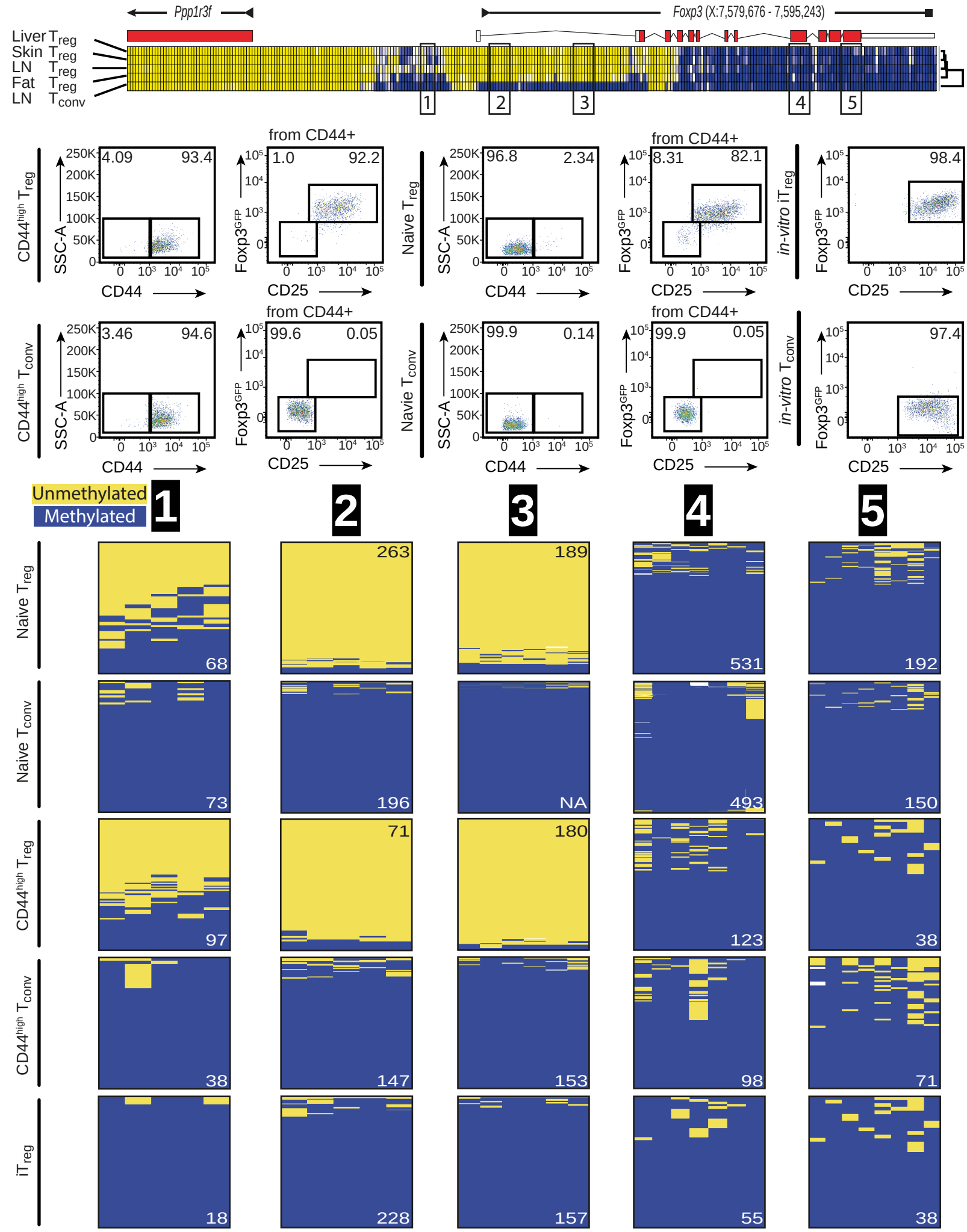

Supplementary Figure 6. Analysis of *Foxp3* CpG methylation in naive or memory T cells. This supplementary figure is an extension of **Figure 3.** On top, overview of *Foxp3* gene methylation status based on TWGBS data. Below, post-sort quality control of target cell populations. From spleen and lymph nodes, we isolated CD44-positive T_{reg} cells ($CD4^+CD8^-CD44^+CD25^+CD25^+Foxp3(GFP)^+$), CD44-positive T_{conv} cells ($CD4^+CD8^-CD44^+CD25^-Foxp3(GFP)^-$), naive T_{reg} cells ($CD4^+CD8^-CD44^-CD25^+Foxp3(GFP)^+$), naive T_{conv} cells ($CD4^+CD8^-CD44^-CD25^-Foxp3(GFP)^-$), *in-vitro* induced T_{reg} cells ($CD4^+CD8^-CD25^+FOXP3(GFP)^+$) and *in-vitro* activated T_{conv} cells ($CD4^+CD8^-CD25^+FOXP3(GFP)^-$). Results of 454 pyrosequencing for all T cell populations and regions are shown below, where colors indicate methylation status of the individual CpG sites. Yellow represents unmethylated and blue methylated CpG, while numbers depict quantity of analyzed reads.

Supplementary Fig. 7

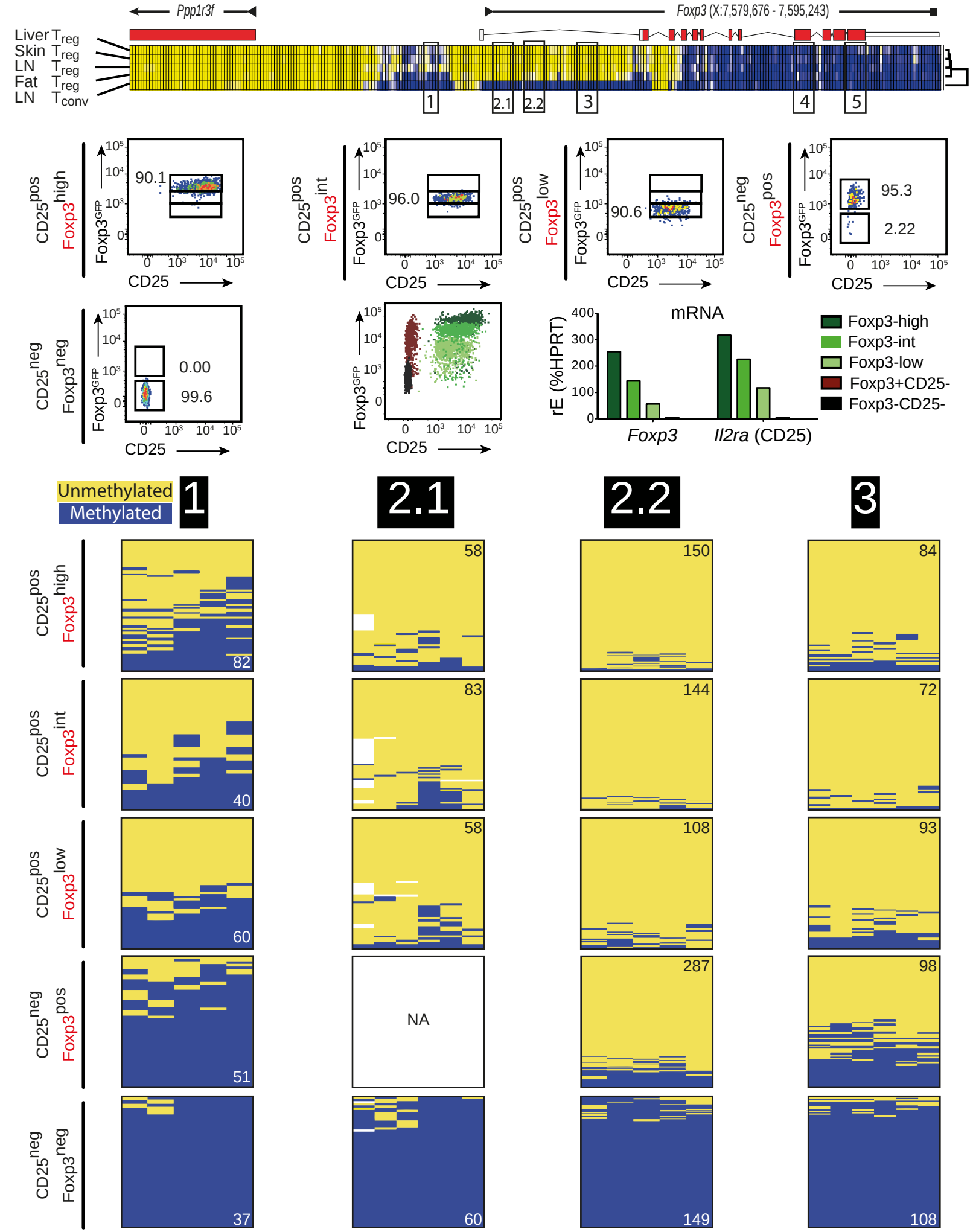

Supplementary Figure 7. Analysis of *Foxp3* CpG methylation in *Foxp3*-high, -medium, -low or *Foxp3*-non expressing T cells. This supplementary figure is an extension of **Figure 3.** On top, overview of *Foxp3* gene methylation status based on TWGBS data. Below, post-sort quality control and RNA expression of target cell populations for *Foxp3* and *Il2ra* (CD25). We isolated $Foxp3^{high}$, $Foxp3^{intermediate}$, and $Foxp3^{low}$ expressing T_{reg} cells ($CD3^+CD4^+CD8^-CD19^-CD25^+Foxp3(GFP)^{high/int/low}$), $CD25^{negative}$ Foxp3-expressing cells ($CD3^+CD4^+CD8^-CD19^-CD25^-Foxp3(GFP)^{pos}$) and T_{conv} cells ($CD3^+CD4^+CD8^-CD19^-CD25^-Foxp3(GFP)^{neg}$). Results of 454 pyrosequencing for all T cell populations and regions are shown below, where colors indicate methylation status of the individual CpG sites. Yellow represents unmethylated and blue methylated CpG, while numbers depict quantity of analyzed reads.

Supplementary Fig. 8

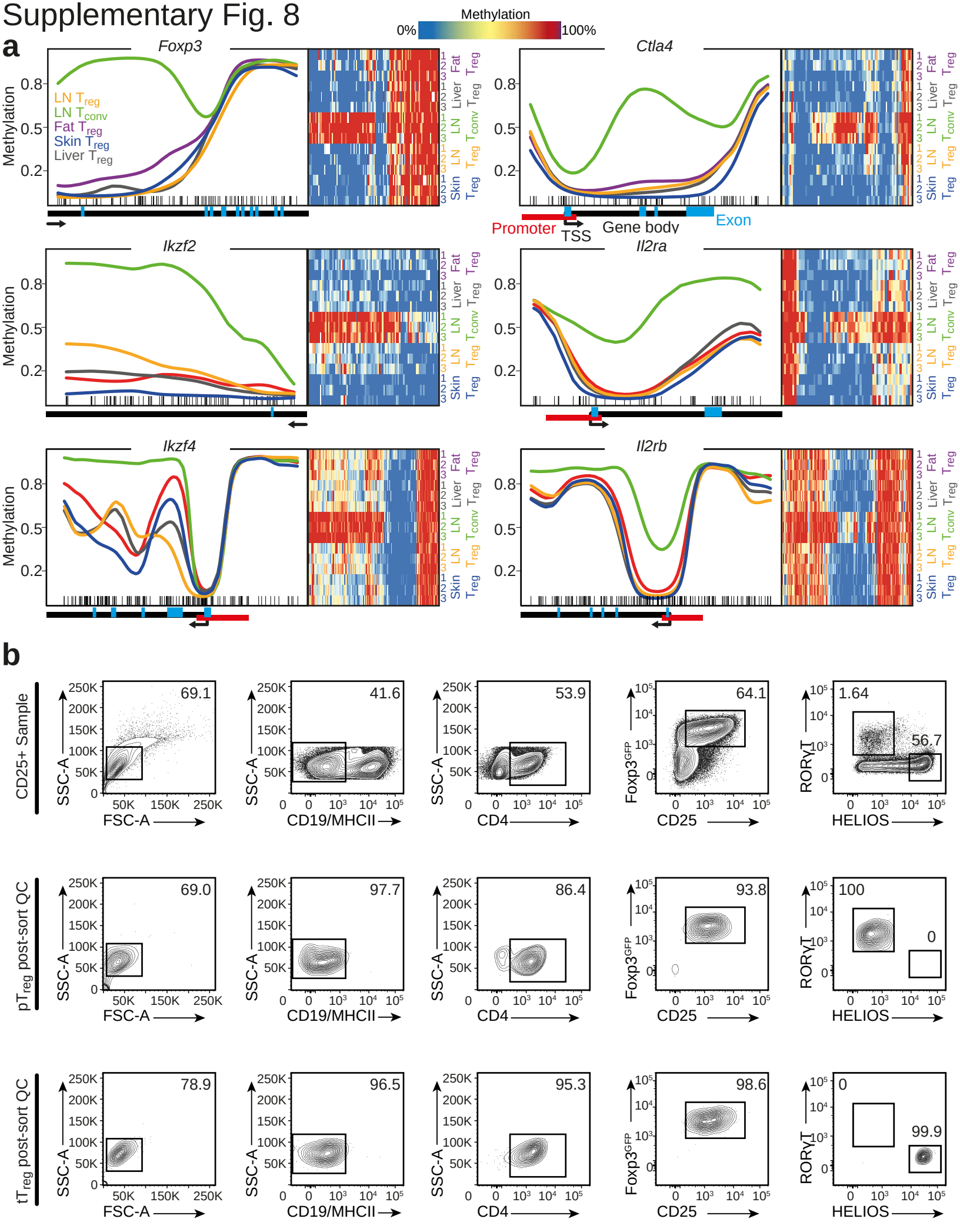

Supplementary Figure 8. Analysis of common thymic T_{reg}-specific demethylated genes in T_{reg} cells and pT_{reg} vs. tT_{reg} post-sort QC. This supplementary figure is an extension of **Figure 3.** (**a**) Methylation plots from three replicates of LN T_{reg} (yellow), LN T_{conv} (green), liver T_{reg} (grey), fat T_{reg} (purple), and skin T_{reg} cells (blue). The left-hand part of each plot is a smoothed graphical representation of CpG methylation (all three replicates averaged). Methylation levels are beta values ranging from 0 (unmethylated) to 1 (methylated). The attached right panel represents the methylation of all individual CpGs, indicated as little ticks at the bottom of each plot, as a heat map for each replicate. The methylation status of the CpGs is indicated by color-code (blue = unmethylated to red = methylated). Gene body, promoter, TSS and exon structures are annotated below the graph. Arrows indicate gene direction, black bars gene body regions, red bars annotated promoter regions, and blue bars exons. The precise genomic localization of the DMR can be found in supplementary Table S1. We plot *Foxp3* (Forkhead box P3), *Ctla4* (Cytotoxic T-lymphocyte-associated protein 4; CD152; Ly-56), *Ikzf2* (IKAROS family zinc finger 2; Helios), *Il2ra* (Interleukin 2 receptor, alpha chain; CD25; Ly-43), *Ikzf4* (IKAROS family zinc finger 4; Eos), *Il2rb* (Interleukin 2 receptor, beta chain; CD122). (**b**) Presort gating scheme for pT_{reg} ($CD4^+CD8^-CD19^-MHCII^-CD25^+Foxp3(GFP)^+HELIOS^-RORgT^+$) and tT_{reg} ($CD4^+CD8^-CD19^-MHCII^-CD25^+Foxp3(GFP)^+HELIOS^+RORgT^-$) cells sorted from CD25 pre-enriched T cells isolated from pooled spleens, including a post-sort re-acquisition of samples for quality control measure. Cells were gated as indicated. Numbers indicate percent of cells per gate.

Supplementary Fig. 9

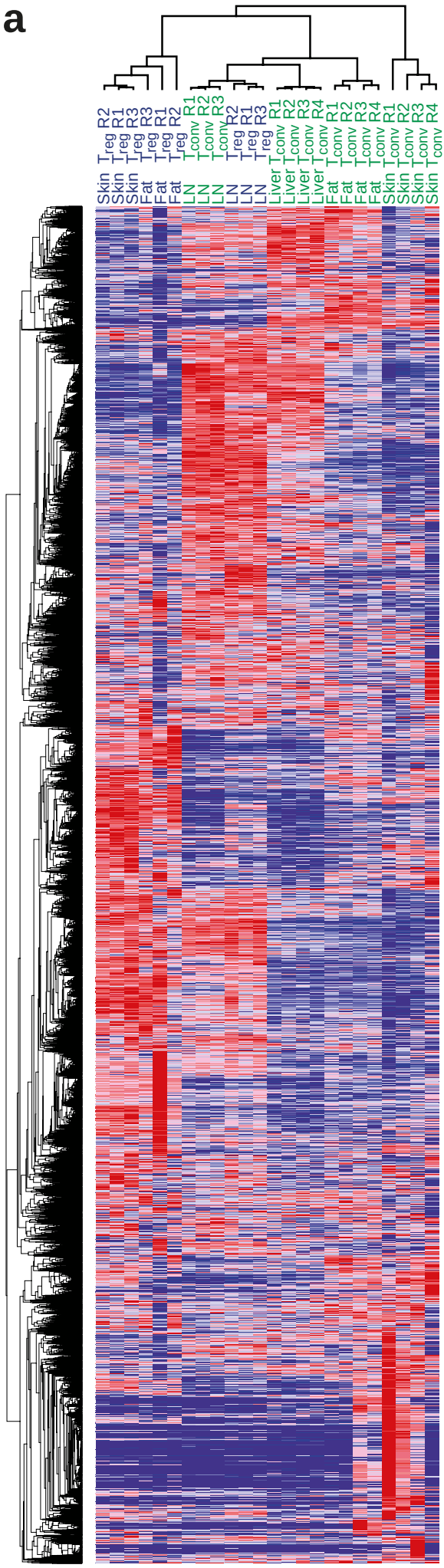

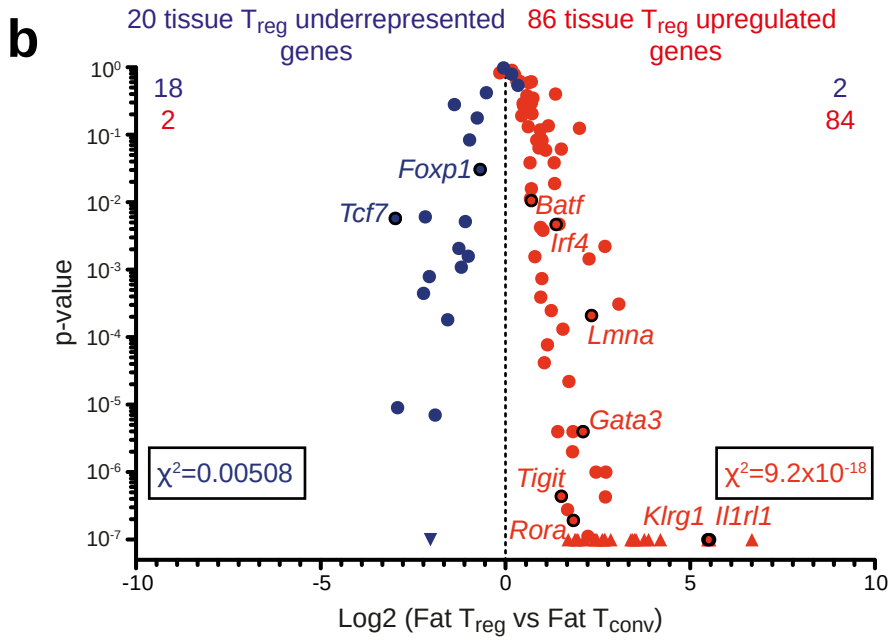

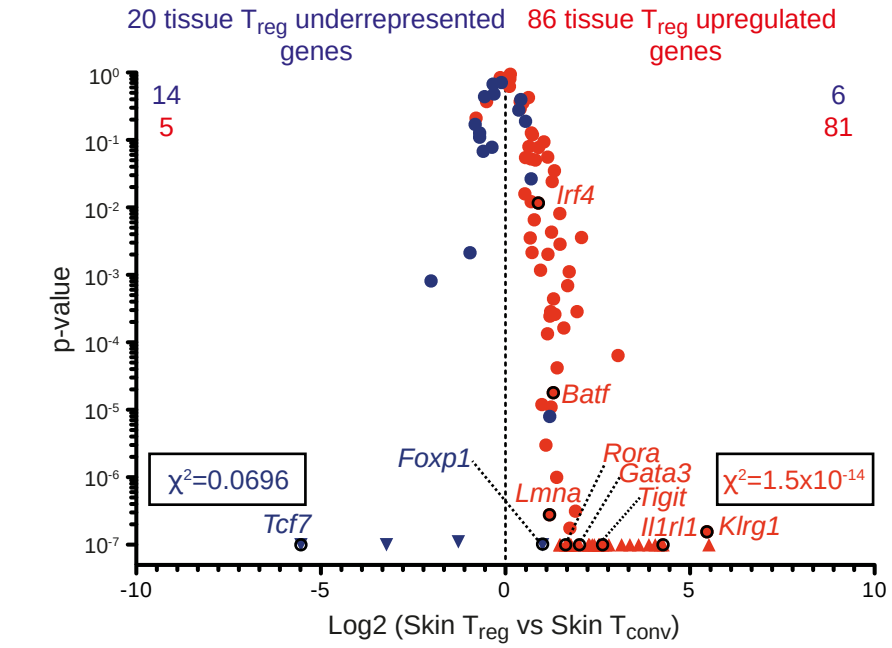

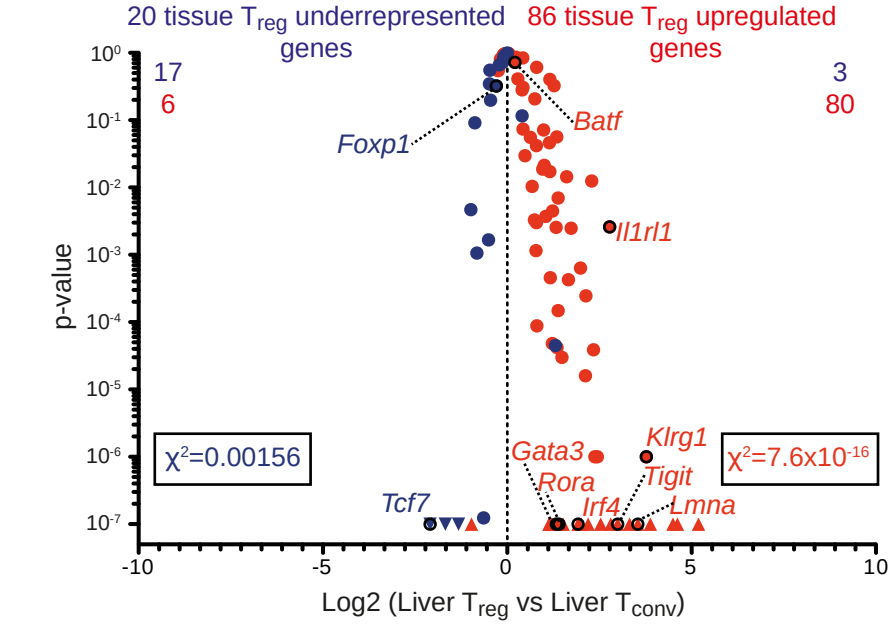

Supplementary Figure 9. Clustering of tissue T_{reg} vs. tissue T_{conv} genes and tissue T_{reg} signature overlay in T_{reg} vs. T_{conv} comparisons. This supplementary figure is an extension of **Figure 4.** (**a**) Hierarchical clustering visualizing the expression of genes in T_{reg} cells isolation from skin, fat, and LN and T_{conv} cells isolated from LN, liver, fat, and skin. Data are RPKM values and hierarchical clustering was performed with gene pattern software. We only plot genes with a cumulated total expression of more than 25 RPKM in all groups (total of 9643 genes are shown). Colors indicate relative gene expression, with red = high and blue = low expression. (**b**) 106 signature genes derived from **Fig.4b** were plotted in the comparison of fat T_{reg} vs fat T_{conv} cells (top), skin T_{reg} vs skin T_{conv} cells (middle), and liver T_{reg} vs liver T_{conv} cells (bottom). Tissue T_{reg} upregulated genes were colored in red (n=86), tissue T_{reg} underrepresented genes in blue (n=20). Numbers indicate number of genes per area. Statistical testing of bias was performed with Chi-Square-testing. Genes with a p-value of $<10^{-7}$ were set to 10^{-7} and formatted with a triangle.

Supplementary Fig. 10

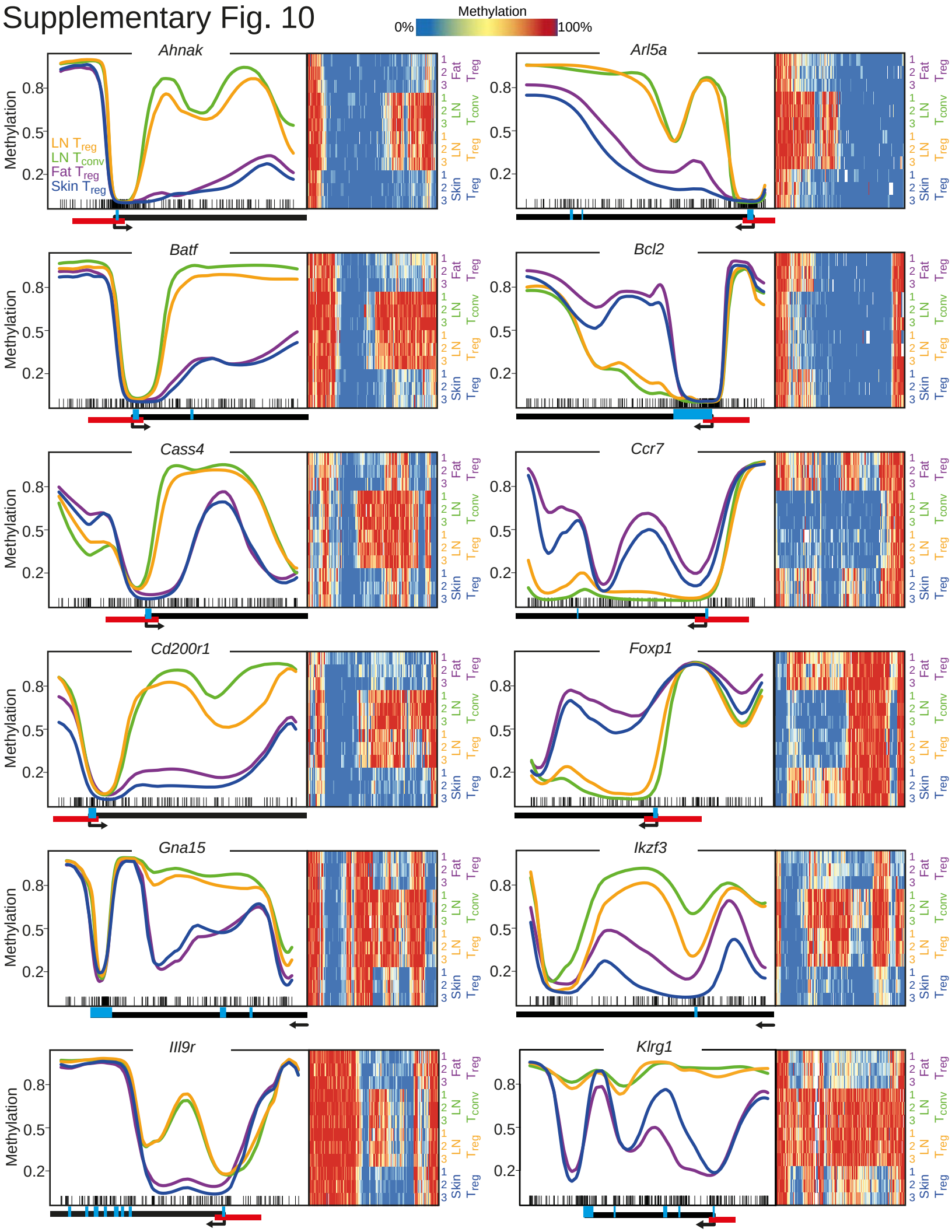

Supplementary Fig. 10

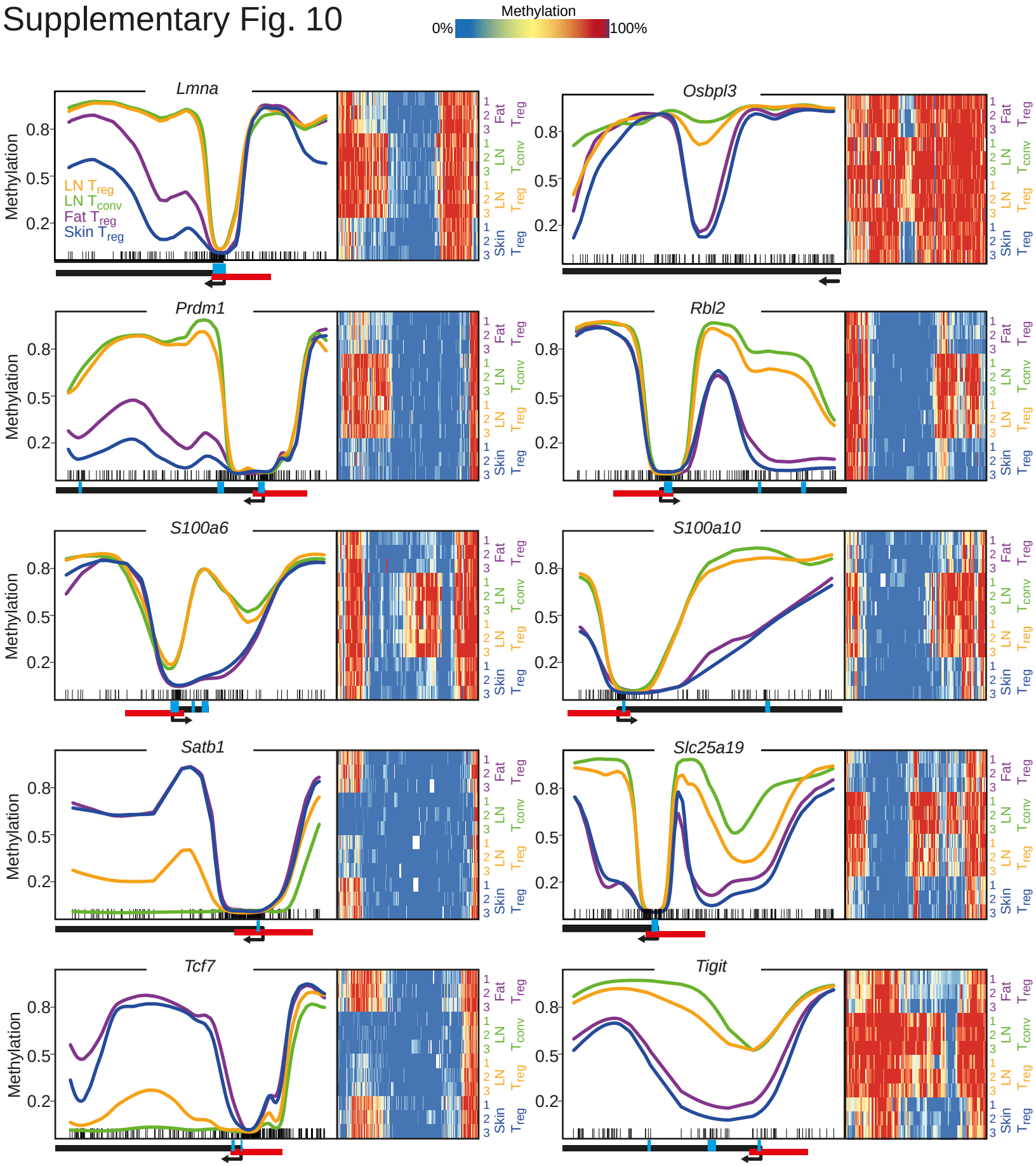

Supplementary Figure 10. Methylation plots of genes differentially methylated in skin and fat T_{reg} vs. LN T_{reg}/LN T_{conv}. This supplementary figure is an extension of **Figure 4.** Methylation plots from three replicates describing genes specifically demethylated or specifically methylated in T_{reg} cells from skin (blue) and fat (purple) tissue vs. LN T_{reg} (yellow) and LN T_{conv} (green) cells. We plot *Ahnak* (Neuroblast differentiation-associated protein), *Arl5a* (ADP-ribosylation factor-like 5A), *Batf* (Basic leucine zipper transcription factor, ATF-like;B-ATF), *Bcl2* (B cell leukemina/lymphoma 2), *Cass4* (Cas scaffolding protein family member 4), *Ccr7* (Chemokine C-C motif receptor 7), *Cd200r1* (CD200 receptor 1; OX2R), *Foxp1* (Forkhead box P1), *Gna15* (Guanine nucleotide binding protein, alpha 15), *Ikzf3* (Ikaros family zinc finger 3), *Il9r* (Il-9 receptor), *Klrg1* (Killer cell lectin-kike receptor subfamily G, member 1; MAFA), *Lmna* (Lamin A), *Osbpl3* (Oxysterol binding protein-like 3), *Prdm1* (PR domain containing 1, with ZNF domain; Blimp1), *Rbl2* (Retinoblastoma-like 2), *S100a6* (S100 calcium binding protein A6), *S100a10* (S100 calcium binding protein A10), *Satb1* (Special AT-rich sequence binding protein 1), *Slc25a19* (Solute carrier family 25(mitochondrial thiamine pyrophosphate carrier), member 19), *Tcf7* (Transcription factor 7, T cell specific; Tcf1), *Tigit* (T cell immunoreceptor with Ig and ITIM domains).

Supplementary Fig. 11

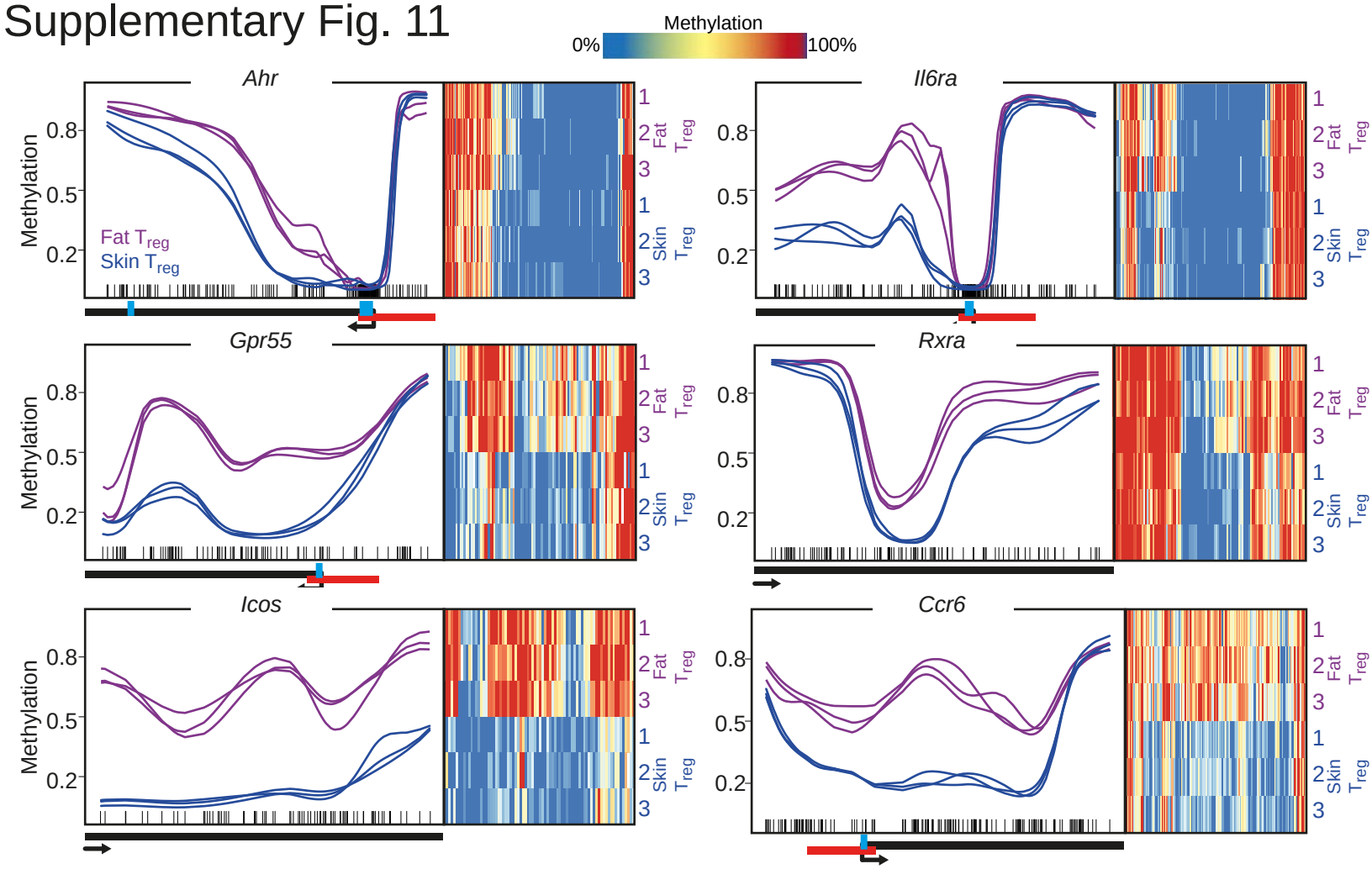

Supplementary Figure 11. Detailed overview of methylated or demethylated regions specific for skin or fat T_{reg} cells. This supplementary figure is an extension of **Figure 5.** Methylation plots of genes specifically demethylated or specifically methylated in T_{reg} cells from skin (blue) or fat (purple) tissue, with three replicates shown for each group. The left-hand part of each plot is a smoothed graphical representation of CpG methylation (individual replicates are shown). Methylation levels are beta values ranging from 0 (unmethylated) to 1 (methylated). The attached right panel represents the methylation heat map of all individual CpGs, indicated as little ticks at the bottom of each plot. The methylation status of the CpGs is indicated by color-code (blue = unmethylated to red = methylated). Gene body, promoter, TSS and exon structures are annotated below the graph. Arrows indicate gene direction, black bars gene body regions, red bars annotate promoter regions, and blue bars exons. We plot *Ahr* (Aryl hydrocarbon receptor), *Il6ra* (Interleukin-6 receptor; CD126), *Gpr55* (G protein-coupled receptor 55; CTFL), *Rxra* (Retinoid X receptor alpha; Nr2b1), *Icos* (Inducible T cell co-stimulator; Ly115), *Ccr6* (Chemokine C-C motif receptor 6).

Supplementary Fig. 12

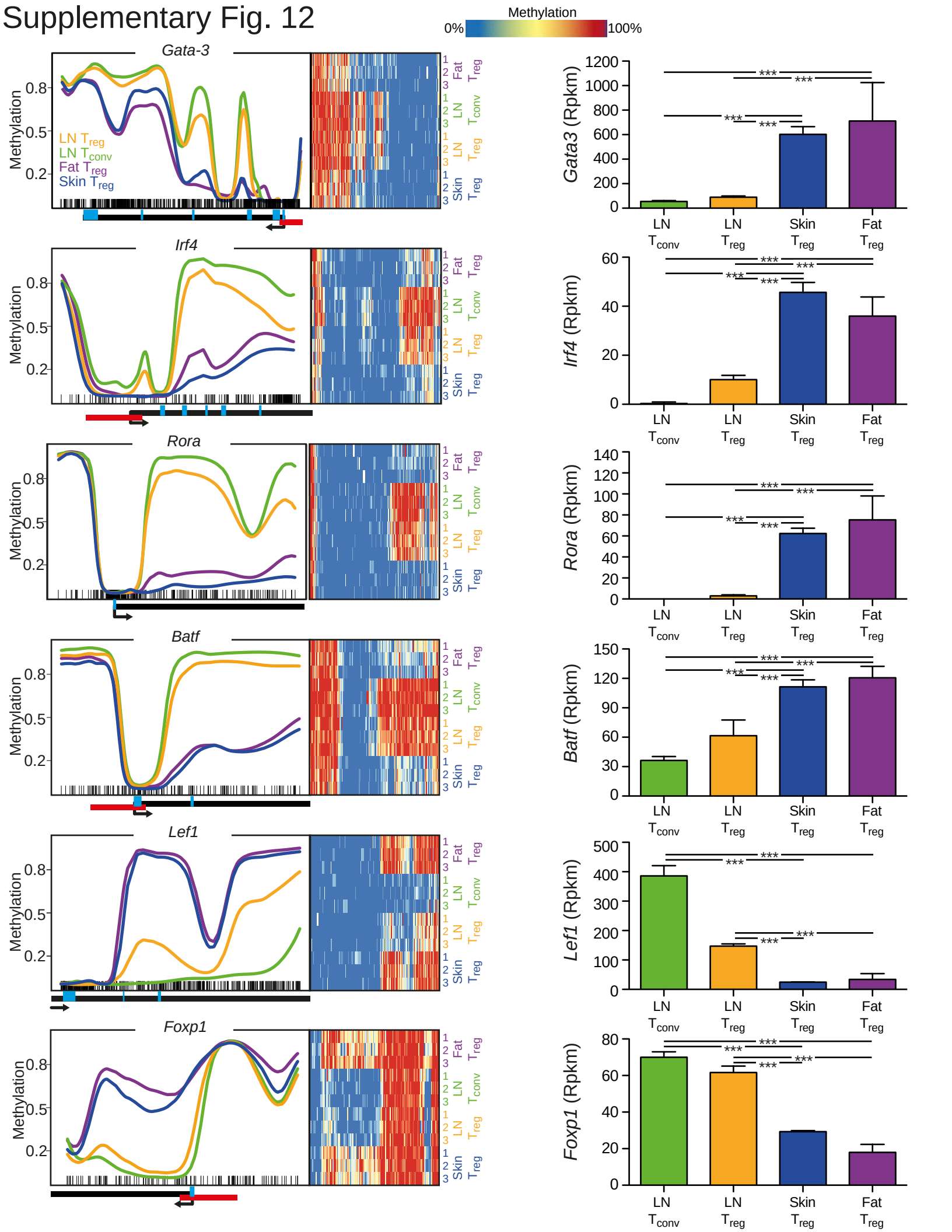

Supplementary Figure 12. Detailed overview of the CpG methylation plus gene expression of *Gata3*, *Irf4*, *Rora*, *Batf*, *Lef1,* and *Foxp1*. This supplementary figure is an extension of **Figure 6**. Methylation plots of three replicates from T_{reg} cells from skin (blue) and fat (purple) tissue vs. LN T_{reg} (yellow) and LN T_{conv} (green) cells. Gene expression is shown to the right of the methylation plots, and statistics are based on RNA sequencing calculations as described in the materials and methods section, with ***=p<0.001. We plot *Gata3*, *Irf4*, *Rora*, *Batf*, *Lef1,* and *Foxp1*.

Supplementary Fig. 13

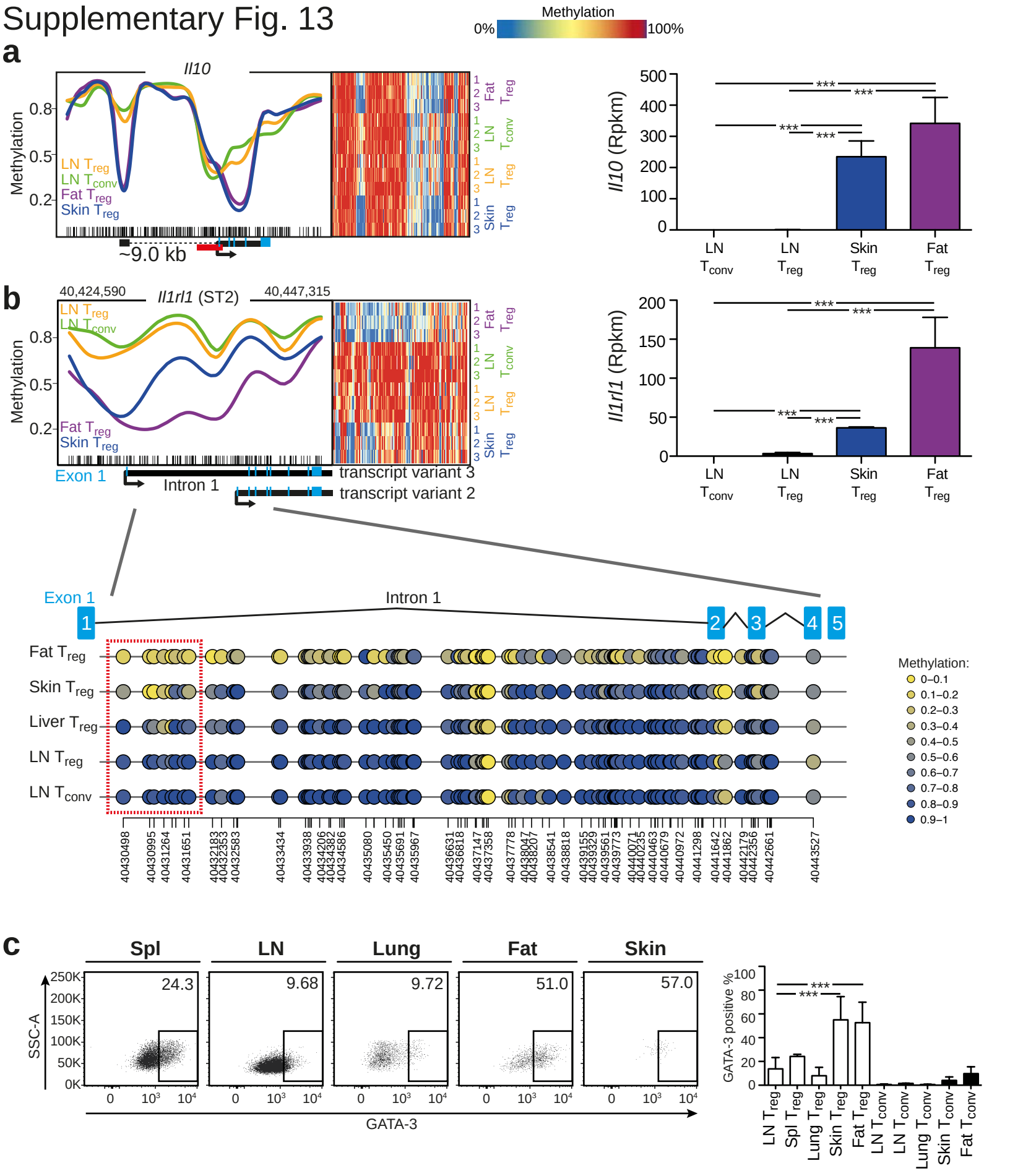

Supplementary Figure 13. Detailed overview of the CpG methylation plus gene expression of *Il10* and *Il1rl1* and GATA-3 expression in tissue T cells. This supplementary figure is an extension of **Figure 6**. (**a** and **b**) Methylation plots from three replicates of T_{reg} cells from skin (blue) and fat (purple) tissue vs. LN T_{reg} (yellow) and LN T_{conv} (green) cells, with (**a**) methylation profile and gene expression of *Il10* (Interleukin 10) and (**b**) methylation footprint of *Il1rl1* (Interleukin 1 receptor-like 1; Interleukin 33 receptor; St2) and its expression. Shown below is a detailed CG analysis of *Il1rl1*. Each circle represents one CpG and the color-code represents degree of methylation from yellow (low) to blue (high). The red box indicates a common tissue T_{reg}-specific demethylated region in *Il1rl1* Intron I. (**c**) Concatenated dot plots of T cells from spleen, lymph node, lung, fat, and skin. GATA-3 expression of pre-gated T_{reg} cells ($CD8^-CD19^-MHCII^-CD3^+CD4^+CD25^+Foxp3^+$) is plotted. Quantification across replicates (n=4-19) is shown to the right in a bar graph. Statistical testing was performed with one-way ANOVA (***=$p<0.001$).

Supplementary Fig. 14

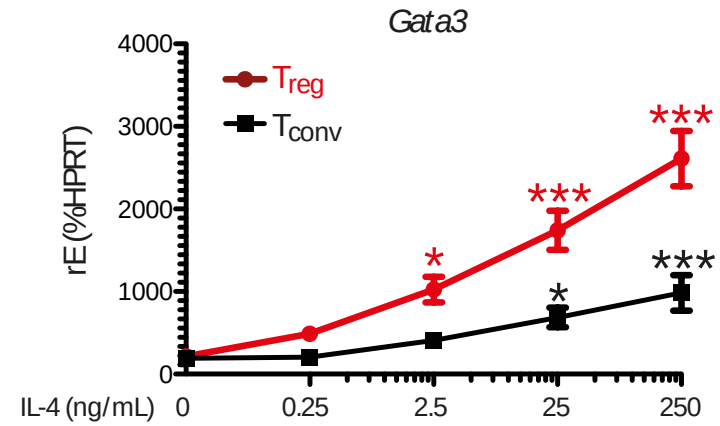

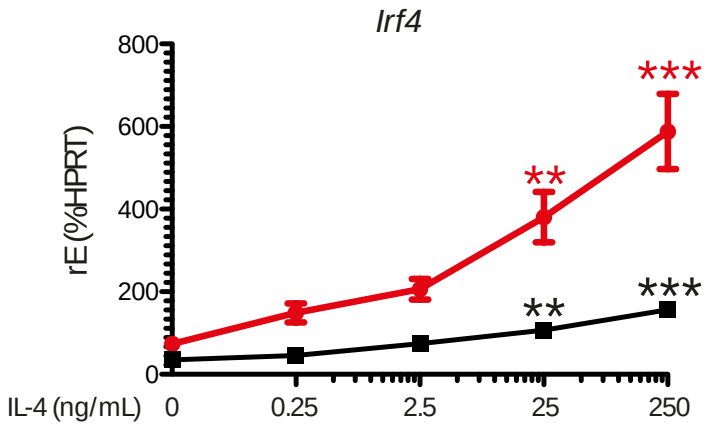

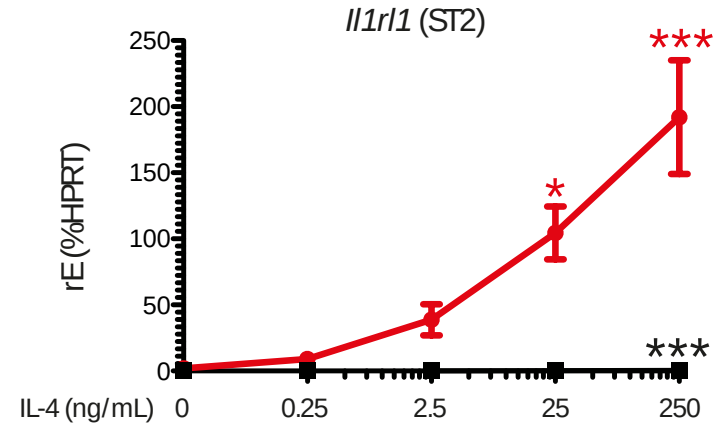

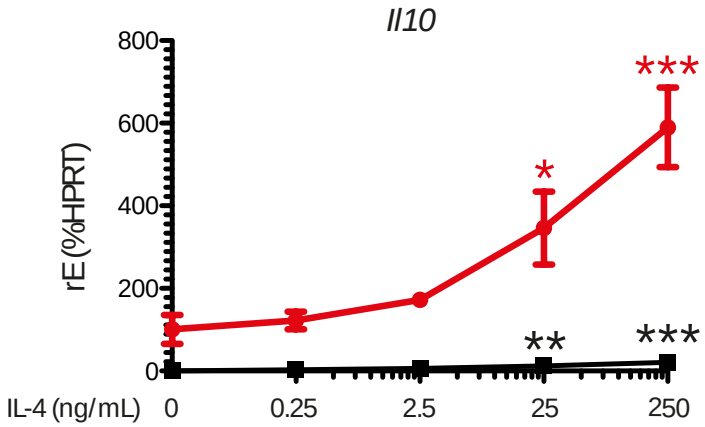

Supplementary Figure 14. Influence of IL-4 on tissue T_{reg} signature induction. This supplementary figure is an extension of **Figure 6**. Primary $CD8^-CD19^-MHCII^-CD3^+CD4^+CD25^+Foxp3^+KLRG1^-ST2^-$ T_{reg} cells (red) and $CD8^-CD19^-MHCII^-CD3^+CD4^+CD25^-Foxp3^-KLRG1^-ST2^-$ T_{conv} cells (black) isolated from spleen and LN were FACS-isolated and cultured with different concentrations of recombinant mouse IL-4. Expression of T_H2-related factors *Gata3*, *Irf4*, *Il1rl1*, and *Il10* was measured by qPCR. IL-4 concentration is shown on the x-axis, with relative expression of the target gene on the y-axis. Statistical analysis is performed against the untreated (0 ng IL-4) sample with one-way ANOVA and Dunnett's post-test to compare all columns vs. control column (***=p<0.001; **=p<0.01; *=p<0.05). Mean and SD of 4 biological replicates are shown.

Supplementary Fig. 15

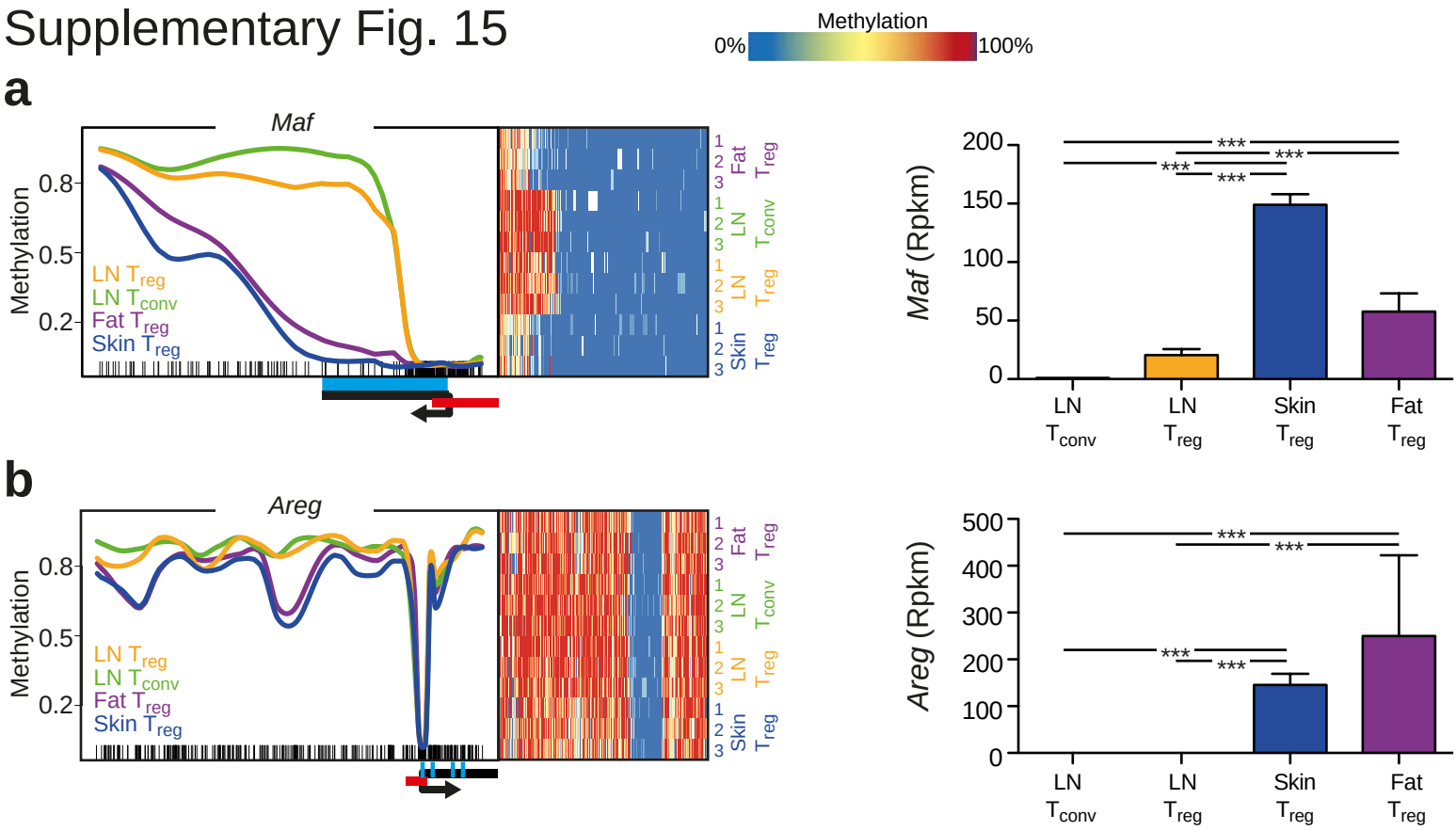

Supplementary Figure 15. Detailed overview of the CpG methylation plus gene expression of *Maf* and *Areg*. Methylation and gene expression profile of *Maf* (**a**) and *Areg* (**b**). Gene expression is shown to the right of the methylation plots, and statistics are based on RNA sequencing calculations as described in the materials and methods section, with ***=p<0.001

Supplementary Fig. 16

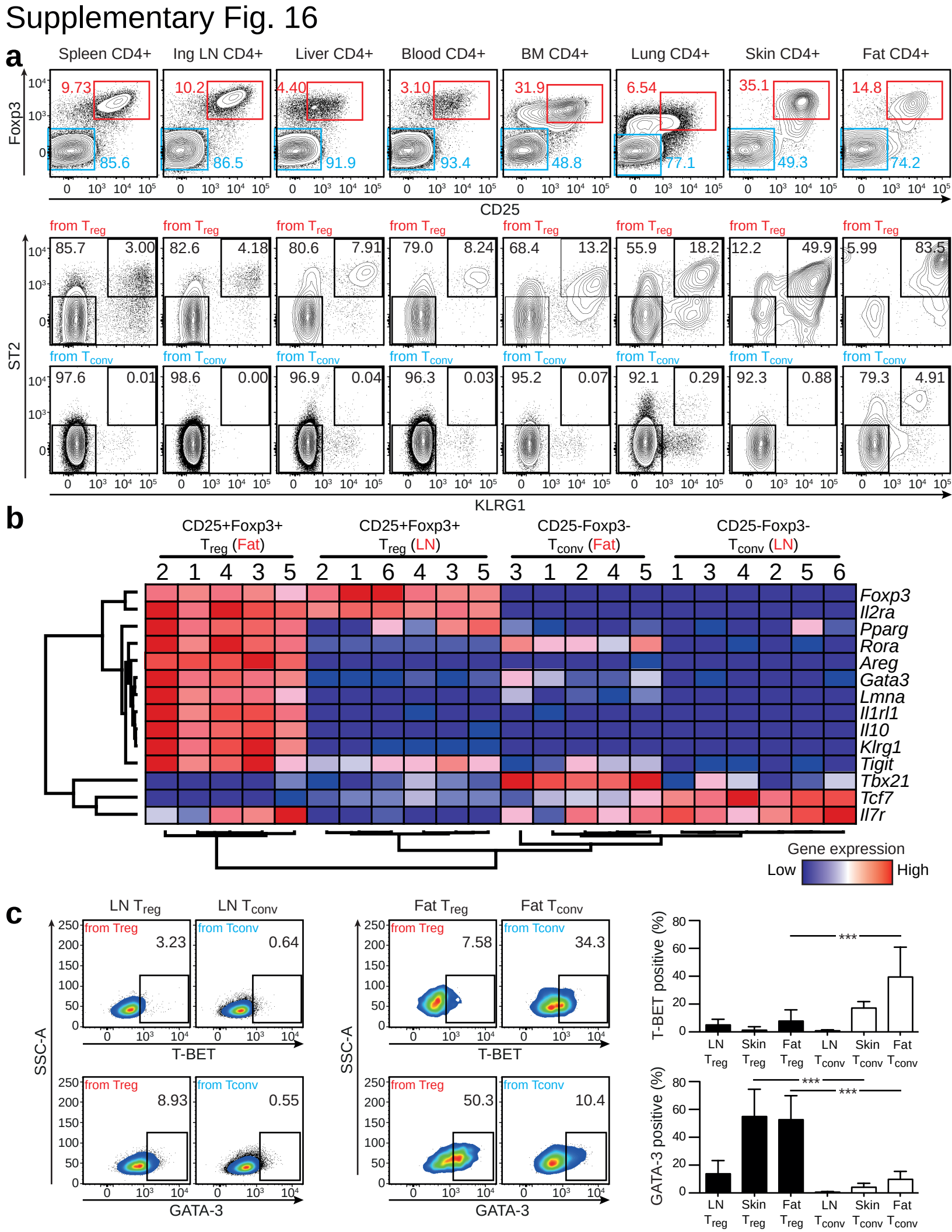

Supplementary Figure 16. tisT_{reg}ST2 marker expression in tissue T_{reg} and T_{conv} cells. This supplementary figure is an extension of **Figure 7.** (**a**) T_{reg} ($CD8^-CD19^-MHCII^-CD3^+CD4^+CD25^+Foxp3^+$, red gate) and T_{conv} ($CD8^-CD19^-MHCII^-CD3^+CD4^+CD25^-Foxp3^-$, blue gate) cells from different tissues (spleen, LN, liver, blood, bone marrow, lung, skin, and fat) were analyzed by flow cytometry. Presence of $KLRG1^+ST2^+$ cells in T_{reg} and T_{conv} compartment is shown below. Dot plots are concatenated files of four biological replicates. In (**b**), T_{reg} cells ($CD45^+CD3^+CD4^+CD8^-CD25^+Foxp3(GFP)^+$) and T_{conv} cells ($CD45^+CD3^+CD4^+CD8^-CD25^-$ $Foxp3(GFP)^-$) from fat and LN have been FACS-isolated and gene expression was measured by real-time PCR. Gene expression data have been subjected to unsupervised hierarchical clustering, and colors indicate relative expression with blue=low and red=high. Six biological replicates for lymph node samples and five biological replicates for fat samples. (**c**) T_{reg} cells ($CD8^-CD19^-MHCII^-CD3^+CD4^+CD25^+Foxp3^+$) and T_{conv} ($CD8^-CD19^-MHCII^-CD3^+CD4^+CD25^-Foxp3^-$) cells from fat and LN were analyzed for the expression of T-BET and GATA-3 by flow cytometry. Dot plots of concatenated files are shown. Quantification for T_{reg} and T_{conv} cells is shown to the right (n=4-19), statistical testing was performed with one-way ANOVA (***=p<0.001).

Supplementary Fig. 17

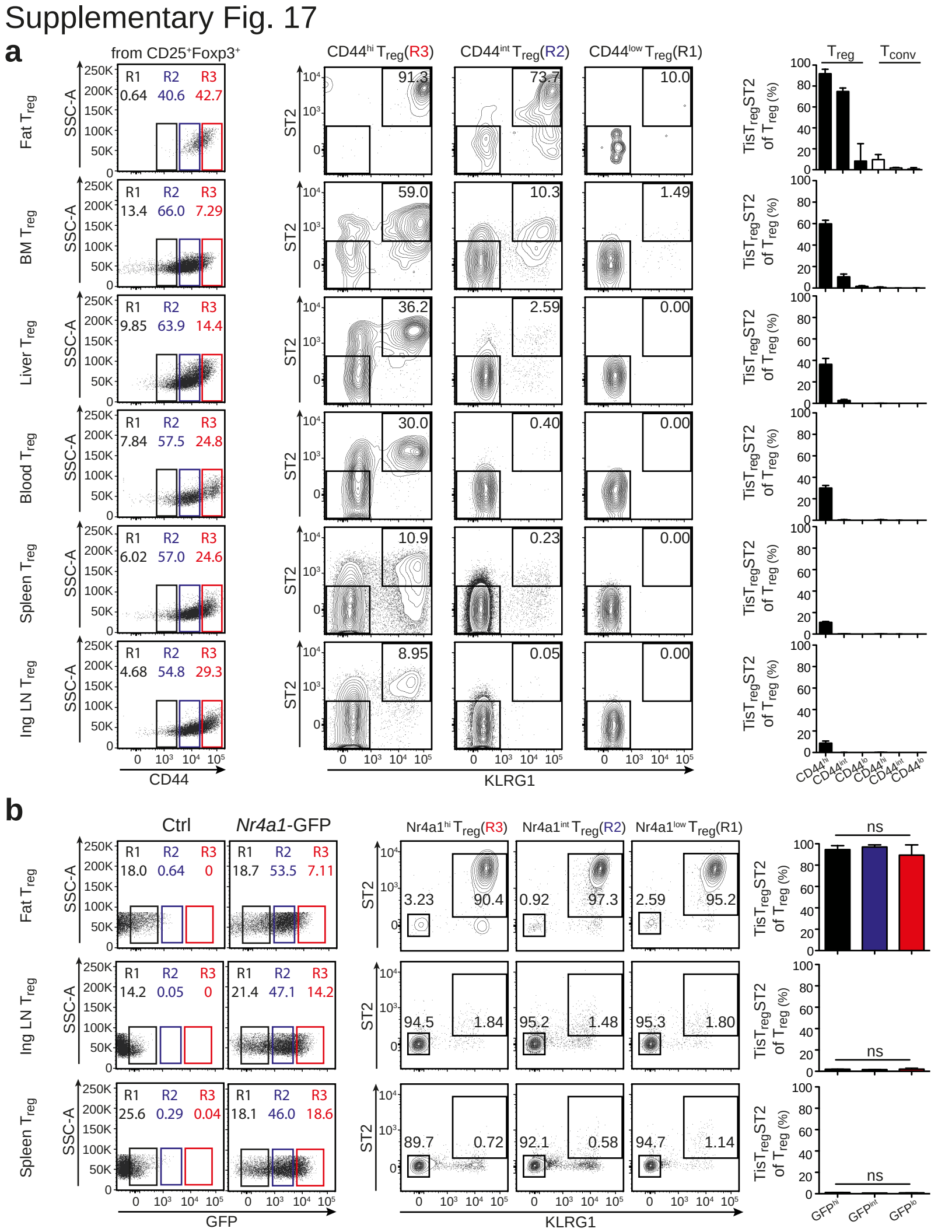

Supplementary Figure 17. CD44 and *Nr4a1*-GFP expression in tisT_{reg}ST2. This supplementary figure is an extension of **Figure 7.** (**a**) T_{reg} cells ($CD8^-CD19^-MHCII^-CD3^+CD4^+CD25^+Foxp3^+$) and T_{conv} ($CD8^-CD19^-MHCII^-CD3^+CD4^+CD25^-Foxp3^-$) cells from different tissues (fat, bone marrow, liver, blood, spleen and LN) were analyzed by flow cytometry. Both T_{reg} and T_{conv} cells were stratified into CD44-high (R3; red gate), CD44-intermediate (R2; blue gate), and CD44-low expressing (R1; black gate) populations, followed by quantification of tisT_{reg}ST2 cells by expression of KLRG1 and ST2. Dot plots of concatenated files are shown. Quantification for T_{reg} and T_{conv} cells is shown to the right (n=4-5). (**b**) T_{reg} cells ($CD8^-CD19^-MHCII^-CD3^+CD4^+CD25^+$) cells from different tissues (fat, LN, and spleen) of *Nr4a1*-GFP reporter mice or reporter negative control mice were analyzed by flow cytometry. T_{reg} cells were stratified into GFP-high (R3, red), GFP-intermediate (R2, blue) or GFP-low (R1, black) populations. These populations were gated for the presence of $KLRG1^+ST2^+$ tisT_{reg}ST2. Dot plots of concatenated files are shown. Quantification is shown to the right and statistical testing was performed with one-way ANOVA (n=4, ns=$p>0.05$).

Supplementary Fig. 18

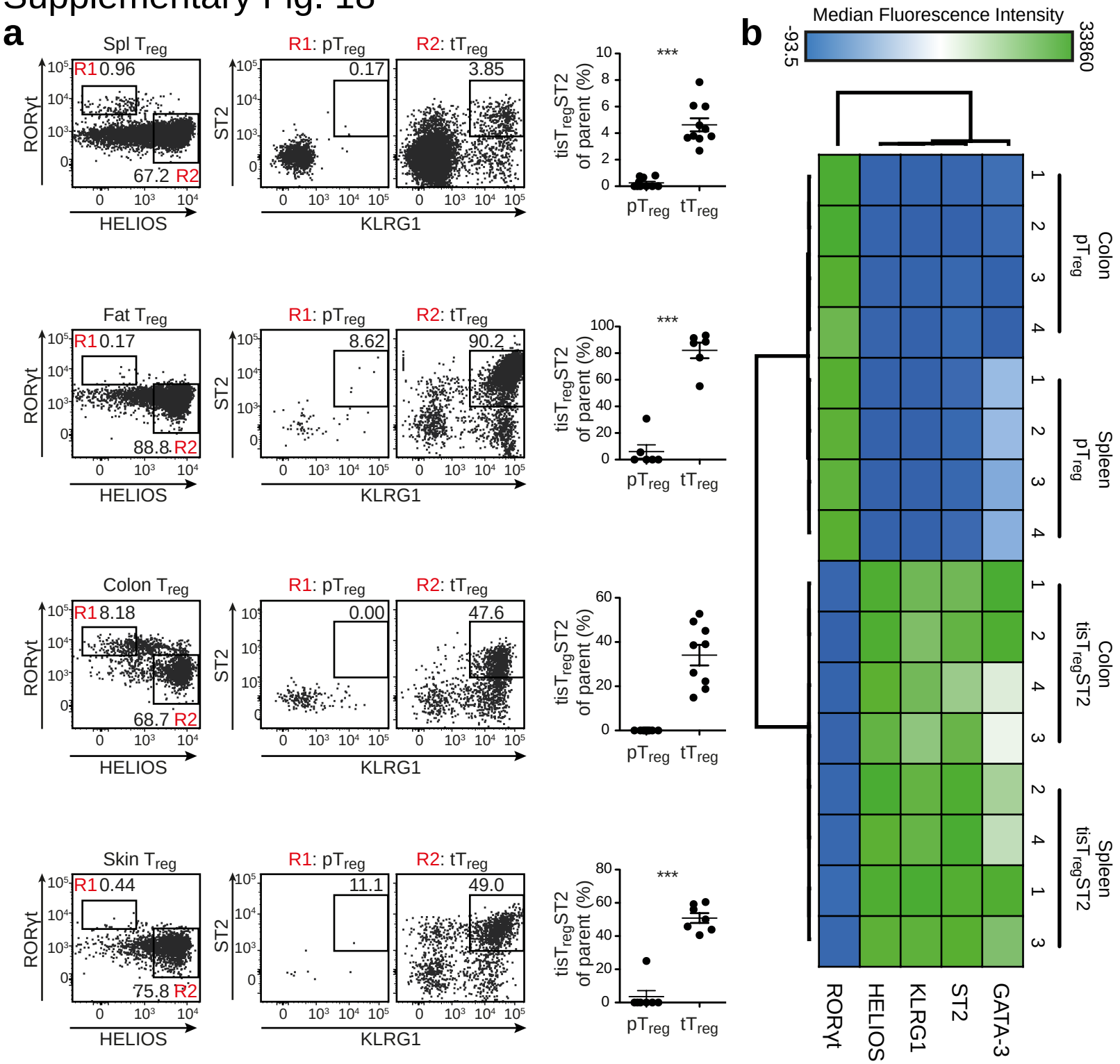

Supplementary Figure 18. Frequency of tisT_{reg}ST2 in the pT_{reg} or tT_{reg} compartment. This supplementary figure is an extension of **Figure 7.** (**a**) T_{reg} cells ($CD8^-CD19^-MHCII^-CD3^+CD4^+CD25^+Foxp3^+$) from spleen, fat, colon and skin were stratified into $ROR\gamma t^+HELIOS^-$ pT_{reg} cells (R1) and $ROR\gamma t^-HELIOS^+$ tT_{reg} cells (R2). Presence of tisT_{reg}ST2 in R1 and R2 was determined, with a statistical quantification shown to the right (two-tailed unpaired student's t test, n=10, ***=p<0.001; in case of colon T_{reg} cells, no statistical testing was possible due to absolute absence of tisT_{reg}ST2 in the pT_{reg} compartment - value of 0). Dot plots are concatenated files of 4 biological replicates. In addition, we stained colon and spleen-derived pT_{reg} and tisT_{reg}ST2 for the expression of GATA-3, ST2, KLRG1, HELIOS, and RORγt in (**b**). Median fluorescence intensity values were derived for each population and visualized in a unsupervised hierarchical cluster. Colors indicate mean fluorescence with green=high and blue=low fluorescence intensity (**b**).

Supplementary Fig. 19

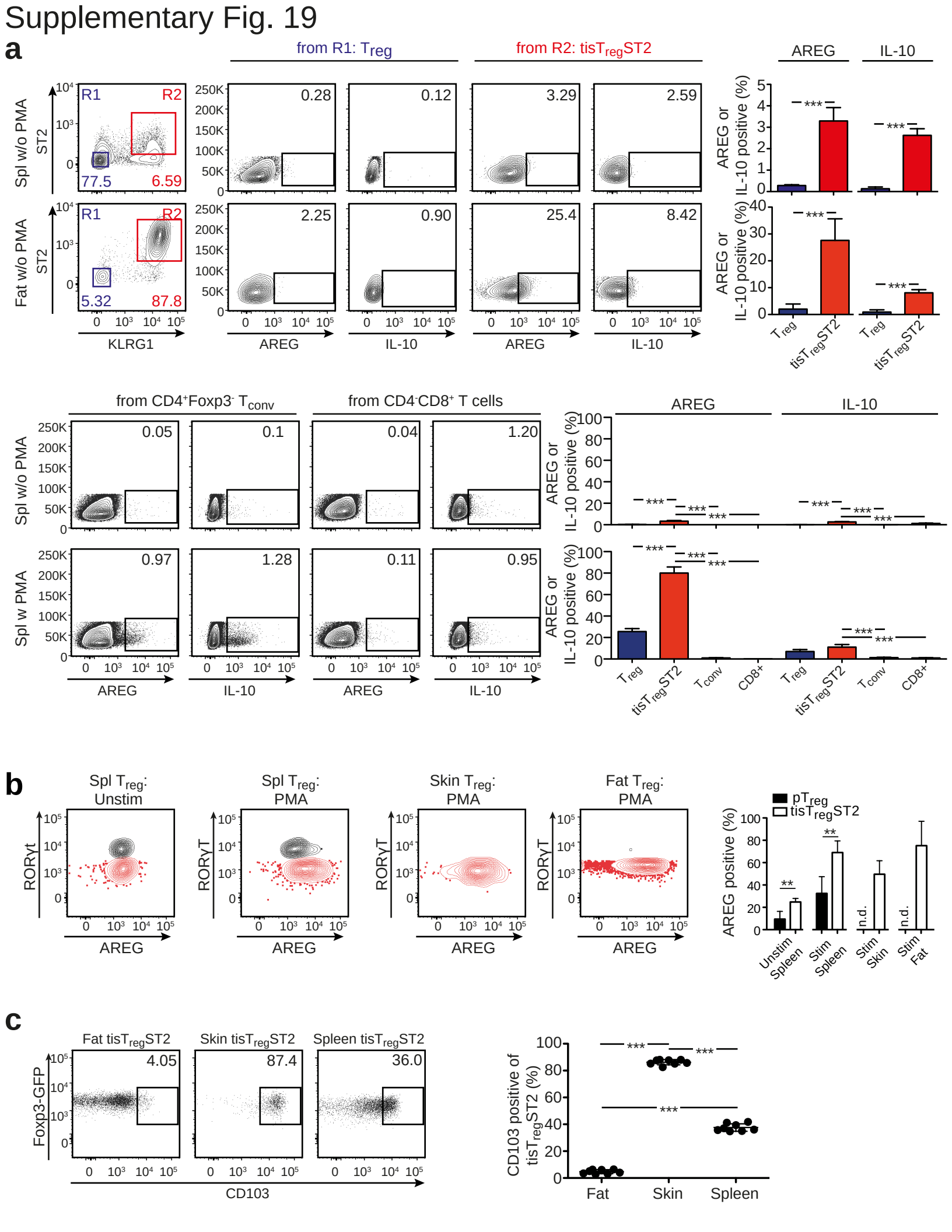

Supplementary Figure 19. Production of AREG and IL-10 in tissue T cells or pT_{reg} vs tT_{reg} and CD103 expression in $tisT_{reg}ST2$. This supplementary figure is an extension of **Figure 7.** (**a**) Spleen or fat cells were stimulated with PMA/Ionomycin (Spl w PMA or Fat w PMA) or left unstimulated (Spl w/o PMA or Fat w/o PMA) in the presence of transport and metalloproteinase inhibitors. $tisT_{reg}ST2$ cells were identified as $CD45^+TCR\beta^+CD4^+CD8^-Foxp3^+KLRG1^+ST2^+$ cells (R2, red) and stained for intracellular expression of AREG and IL-10. As control, we used $KLRG1^-ST2^-$ T_{reg} cells (R1, blue). Quantification is shown to the right. This is the unstimulated control to data shown in **Figure 7d**. In the lower graph, T_{conv} cells were identified as $CD45^+TCR\beta^+CD4^+CD8^-Foxp3^-$ cells and CD8 T cells were identified as $CD45^+TCR\beta^+CD4^-CD8^+Foxp3^-$ cells and stained for intracellular expression of AREG and IL-10. Quantification is shown to the right. Statistical evaluation for all bar graphs was performed with unpaired two-tailed student's t tests (n=4, ***=p<0.001 and *=p<0.05). (**b**) Spleen, skin or fat cells were stimulated with PMA/Ionomycin (PMA) or left unstimulated (Unstim) in the presence of transport and metalloproteinase inhibitors. T_{reg} cells ($CD8^-CD19^-MHCII^-CD3^+CD4^+CD25^+Foxp3^+$) were stratified into $ROR\gamma t^+$ pT_{reg} cells (black color) and $ROR\gamma t^-$ tT_{reg} cells (red color) and expression of AREG was evaluated by intracellular protein staining. Quantification is shown to the right. Statistical evaluation for all bar graphs was performed with unpaired two-tailed student's t tests (n=10, **=p<0.01 and n.d. = not detectable). (**c**) $TisT_{reg}ST2$ cells in fat, skin and spleen were identified as $CD8^-CD19^-MHCII^-CD3^+CD4^+CD25^+Foxp3^+KLRG1^+ST2^+$ and stained for the expression of CD103 by flow cytometry. Concatenated dot plots of CD103 vs. *Foxp3*-GFP staining is shown, with a statistical evaluation to the right. Statistical testing was performed with one-way ANOVA (n=8, ***=p<0.001).

Supplementary Fig. 20

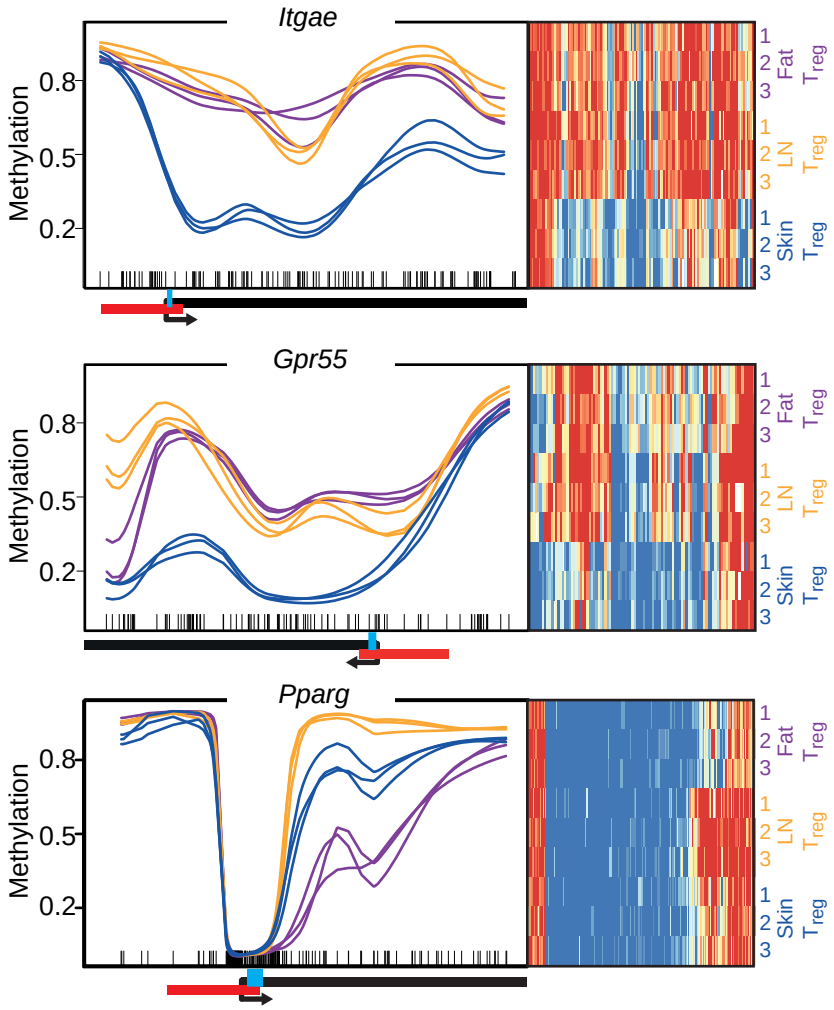

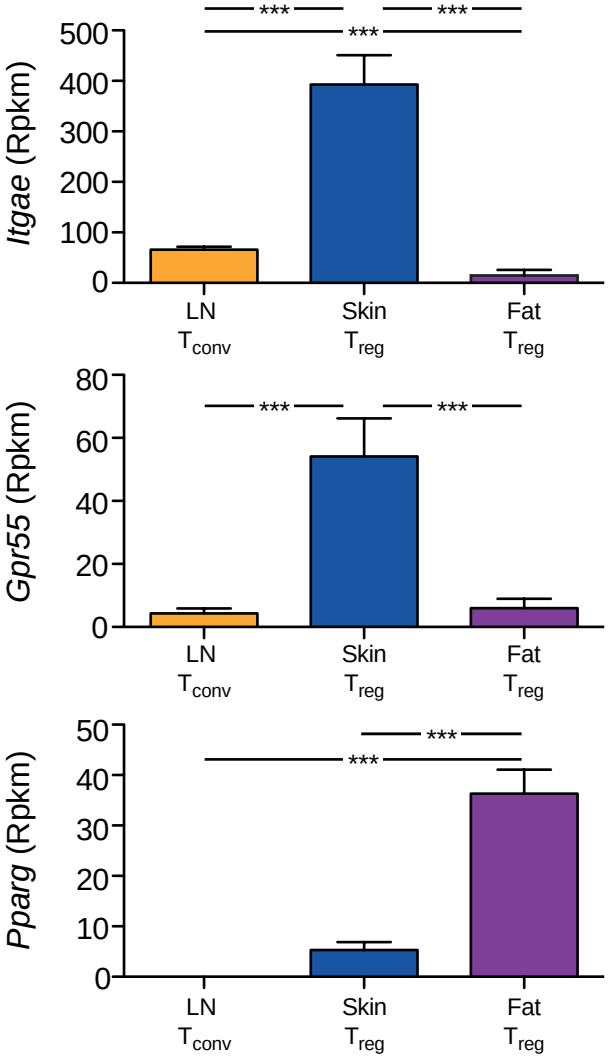

Supplementary Figure 20. Detailed overview of the CpG methylation plus gene expression of *Itgae, Grp55* and *Pparg*. Methylation plots of three replicates from T_{reg} cells from skin (blue), fat (purple) tissue vs. LN (yellow) cells. Gene expression is shown to the right of the methylation plots, and statistics are based on RNA sequencing calculations as described in the materials and methods section, with ***=p<0.001. We plot *Itgae, Gpr55,* and *Pparg.*

Supplementary Fig. 21

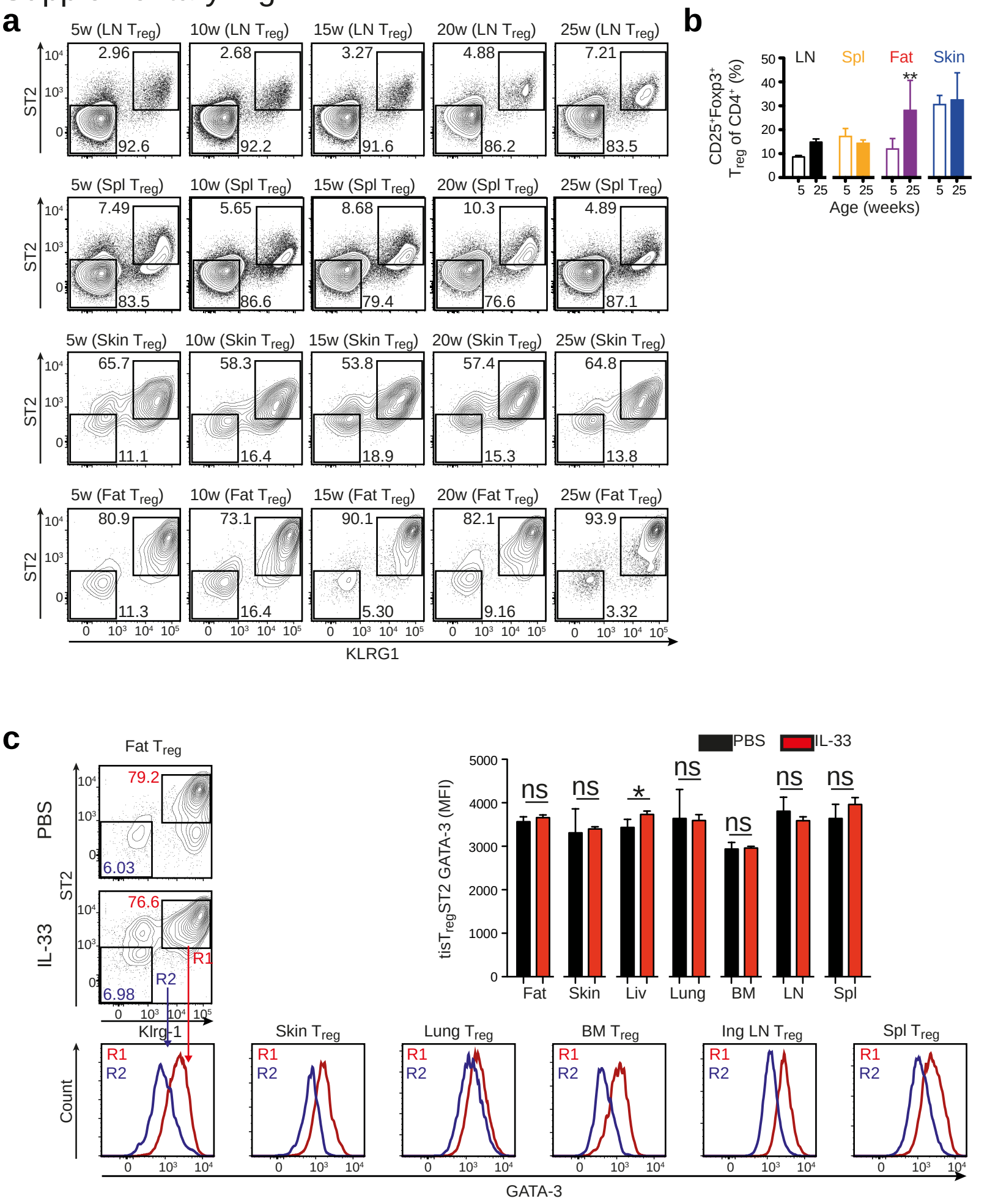

Supplementary Figure 21. Kinetics of tisT_{reg}ST2 and GATA-3 expression in IL-33 expanded tisT_{reg}ST2. This supplementary figure is an extension of **Figure 8.** (**a**) tisT_{reg}ST2 cells from LN, spleen, skin and fat of 5, 10, 15, 20, and 25 week (w) old mice were identified as $CD8^-CD19^-MHCII^-CD3^+CD4^+CD25^+Foxp3^+KLRG1^+ST2^+$ cells. Dot plots are concatenated files of five biological replicates. (**b**) Frequency of T_{reg} cells per $CD4^+$ T cells for LN, spleen, skin and fat of 5 and 25 week old mice. Statistical testing with unpaired two-tailed student's t tests (n=5, **=p<0.01). (**c**) tisT_{reg}ST2 cells have been expanded using IL-33 *in-vivo*, as shown in **Figure 8d**. Expression of GATA-3 in IL-33 expanded $KLRG1^+ST2^+$ tisT_{reg}ST2 (R1, red) and $KLRG1^-ST2^-$ T_{reg} cells (R2, blue) is shown in histograms. Dot plots are concatenated files of four biological replicates. Bar graph, comparison of GATA-3 mean fluorescent intensity (MFI) of tisT_{reg}ST2 expanded (red, IL-33) or under stead-state (black, PBS). Statistical evaluation for bar graphs was performed with unpaired two-tailed student's t tests (n=4, *=p<0.05 and ns=p>0.05).

Supplementary Table 1. Genomic location of DMRs plus/minus 5000 bp. All DMRs mentioned in this manuscript are listed in the table. The genomic location is derived from DMR start and end plus/minus 5000bp extension. The coordinates are based on the Mm10 mouse genome.

Figure #	Gene	Chromosome	Start (Mm10)	End (Mm10)
Figure 3+S2	*Ctla4*	1	60,907,374	60,918,501
Figure 3+S2	*Foxp3*	X	7,578,800	7,590,009
Figure 3+S2	*Il2ra*	2	11,640,082	11,650,987
Figure 3+S2	*Il2rb*	15	78,486,544	78,501,342
Figure 3+S2	*Ikzf2*	1	69,673,872	69,684,278
Figure 3+S2	*Ikzf4*	10	128,638,716	128,650,358
Figure 4+S3	*Ahnak*	19	8,986,548	8,998,035
Figure 4+S3	*Bcl2*	1	106,704,222	106,717,188
Figure 4+S3	*Cd200r1*	16	44,763,971	44,777,159
Figure 4+S3	*Klrg1*	6	122,265,597	122,287,833
Figure 4+S3	*Lmna*	3	88,496,629	88,507,545
Figure 4+S3	*Osbpl3*	6	50,394,775	50,405,730
Figure 4+S3	*Tcf7*	11	52,274,122	52,286,693
Figure 4+S3	*Tigit*	16	43,656,234	43,667,829
Figure 5+S7	*Pparg*	6	115,357,387	115,368,510
Figure 5+S4+S7	*Gpr55*	1	85,953,304	85,964,859
Figure 5+S7	*Itgae*	11	73,088,541	73,101,203
Figure 6+S5	*Areg*	5	91,101,935	91,146,584
Figure 6+S5	*Gata3*	2	9,854,746	9,880,440
Figure 6+S5	*Irf4*	13	30,746,243	30,756,945
Figure 6+S5	*Rora*	9	69,286,853	69,300,249
Figure 6+S5	*Batf*	12	85,683,386	85,694,246
Figure 6+S5	*Il1rl1*	1	40,424,590	40,435,498
Figure 6+S5	*Il10*	1	131,005,084	131,030,000
Figure S2	*Ccr6*	17	8,236,244	8,249,012
Figure S2	*Cish*	9	107,294,631	107,306,431
Figure S2	*Cox10*	11	63,984,483	63,996,993
Figure S2	*Dusp4*	8	34,808,142	34,819,785
Figure S2	*Fam78a*	2	32,068,662	32,080,820
Figure S2	*Ift80*	3	68,997,644	69,008,326
Figure S2	*Itk*	11	46,379,566	46,390,401
Figure S2	*Satb1*	17	51,798,009	51,808,899
Figure S2	*Tgfbr2*	9	116,163,952	116,178,063
Figure S2	*Tnfrsf1b*	4	145,238,372	145,249,492
Figure S2	*Tnfrsf18*	4	156,022,557	156,033,915
Figure S2	*Tnfrsf4*	4	156,009,088	156,022,548

Figure S3	*Arl5a*	2	52,414,045	52,425,469
Figure S3	*Batf*	12	85,683,386	85,694,246
Figure S3	*Cass4*	2	172,389,466	172,401,282
Figure S3	*Ccr7*	11	99,146,768	99,157,822
Figure S3+S5	*Foxp1*	6	99,260,781	99,271,248
Figure S3	*Gna15*	10	81,500,930	81,511,151
Figure S3	*Ikzf3*	11	98,469,112	98,480,270
Figure S3	*Il9r*	11	32,191,379	32,204,333
Figure S3	*Prdm1*	10	44,449,642	44,461,617
Figure S3	*Rbpl2*	8	91,066,494	91,077,384
Figure S3	*S100a6*	3	90,608,349	90,619,399
Figure S3	*S100a10*	3	93,553,297	93,563,730
Figure S3	*Satb1*	17	51,825,368	51,835,842
Figure S3	*Slc25a19*	11	115,624,778	115,635,732
Figure S4	*Ahr*	12	35,526,008	35,536,839
Figure S4	*Ccr6*	17	8,232,518	8,245,115
Figure S4	*Icos*	1	60,982,648	60,993,312
Figure S4	*Il6ra*	3	89,906,495	89,917,344
Figure S4	*Rxra*	2	27,724,547	27,735,775
Figure S5	*Lef1*	3	131,111,109	131,121,822
Figure S5	*Maf*	8	115,696,798	115,707,854